



琉球大学学術リポジトリ

University of the Ryukyus Repository

Title	Numerical stress and fault simulation of Shillong Plateau and its adjoining area in Northeast India, Bangladesh and Myanmar
Author(s)	Islam, Md. Shofiquul; Hayashi, Daigoro
Citation	琉球大学理学部紀要 = Bulletin of the College of Science. University of the Ryukyus(89): 27-58
Issue Date	2010-03
URL	http://hdl.handle.net/20.500.12000/17407
Rights	

Numerical stress and fault simulation of Shillong Plateau and its adjoining area in Northeast India, Bangladesh and Myanmar

Md. Shofiquul Islam and Daigoro Hayashi

Simulation Tectonics Laboratory Faculty of Science, University of the Ryukyus Okinawa, 903-0213, Japan

Abstract

The Shillong Plateau, NE India is reported to be one of the most seismically active 'pop-up' structures lying between the Dauki fault and recently reported Oldham fault in northeast India. Dauki fault lies down faulted Bengal basin to the south and Oldham fault, the Assam valley, the Himalayan foothills region, lesser Himalaya and Butan and Tibet further north. We examined convergent displacement due to northward movement of the Indian plate with respect to the Eurasian plate and also consider uplift of the Plateau simultaneously. Four models with different boundary conditions under both plane strain and plane stress have been selected. The maximum compressive stress shows a preferred orientation that helps us to explain the tectonic environment as well as the fault pattern in plane strain condition. The realistic regional maximum horizontal compressive stress (σ_{Hmax}) orientation is observed within the best-fit model under plane stress condition. The best-fit model result under plane strain condition shows that the compressive stress regime is dominant in the study area, except for the uppermost part of the crust where the tensional stress is dominant. These tensional stress regimes support normal faulting and structural discontinuities. With increase progressive convergent displacement (under plane strain condition), the principal stresses rotate anticlockwise around the fault zones, and the upper crust of the Bengal basin and the Assam valley, on the other hand, behave thrust faulting. Rock properties (density, Poisson's ratio, Young's modulus, cohesion, angle of internal friction) and Mohr-Coulomb failure criterion are used to calculate failure and faulting pattern. The simulated results have significant explanation on the proposed Oldham fault as well as on the geologically evidenced Dauki fault. Our preferred model explains deformation and seismic activity of the area. Our plane stress simulation results show that the Dauki fault is the major controlling element for overall distribution of regional stress, and it accommodates ~25% horizontal displacement. Our plane strain model further suggests that plate convergence is the *driving force* for pop-up tectonics of the Shillong Plateau, and also for deformation in the Shillong Plateau and adjoining area within the crust (<30 km).

Key words: Shillong Plateau, pop-up, numerical simulation, Oldham fault, stress.

1. Introduction

The Shillong Plateau, a part of the Indian shield with an average 1 km elevation, which is separated from the Bangladesh (Bengal basin) by the ~ 300 km long E-W Dauki fault in south and by the Brahmaputra river valley from the Himalaya in north (Kayal, 2001). The Shillong Plateau area is seismically active, tectonically complex and was the epicenter of 1897 Shillong earthquake M 8.7 (Fig.1). Oldham (1899) made a

detailed investigation on the 1897 earthquake and suggested that earthquake was caused by a north dipping thrust fault. Recently, Bilham and England (2001), however, argued that the 1897 earthquake occurred by 'pop up' tectonics of the plateau between the south dipping Oldham fault and north dipping Dauki fault, and the earthquake was caused by a slip of 11m a south dipping Oldham fault. Based on geodetic data, uplift of the SP has been reported by Kailasam (1979) and Das et al. (1995), and it is suggested that the

uplift is balanced by subsidence of the Sylhet trough to the south of the Dauki fault, which is evident by about 18 km thick Tertiary sediments of the Bengal basin (Khan and Agarwal, 1993).

Bilham and England (2001) reported the Oldham fault at the northern boundary of the Shillong Plateau as a blind reverse fault with a length of ~110 km, which dips 57° SSW, extending from 9 to 45 km beneath the Shillong Plateau. On the other hand, Oldham (1899), Chen and Molar (1990), Kayal and De (1991) suggested that the 1897 earthquake occurred due to a north dipping fault at the southern boundary of the plateau. Kayal and De (1991) and Kayal (2001), based on microearthquake surveys data, suggested that the Dapsi thrust, an extension of the Dauki fault to the NW could be the causative fault for seismic activity in

the Shillong Plateau. Rajendran et al. (2004), Kayal et al. (2006) and Nayak et al. (2008) have proposed that the Brahmaputra fault, the E-W segment of the Brahmaputra river could be the northern boundary fault of the plateau, which is around 20 km north of the proposed Oldham fault. Based on recent broadband seismological data, Kayal et al. (2006) further suggested that north dipping NW-SE trending Dapsi thrust, a conjugate NW trending thrust fault of the E-W trending Dauki fault, is the southern boundary of the pop-up tectonics (Fig.1). Several authors argued that neither the surface geological data nor the subsurface geophysical data conform to the presence of the Oldham fault (e.g. Rajendran et al, 2004; Srinivasan, 2003; Kayal et al., 2006.).

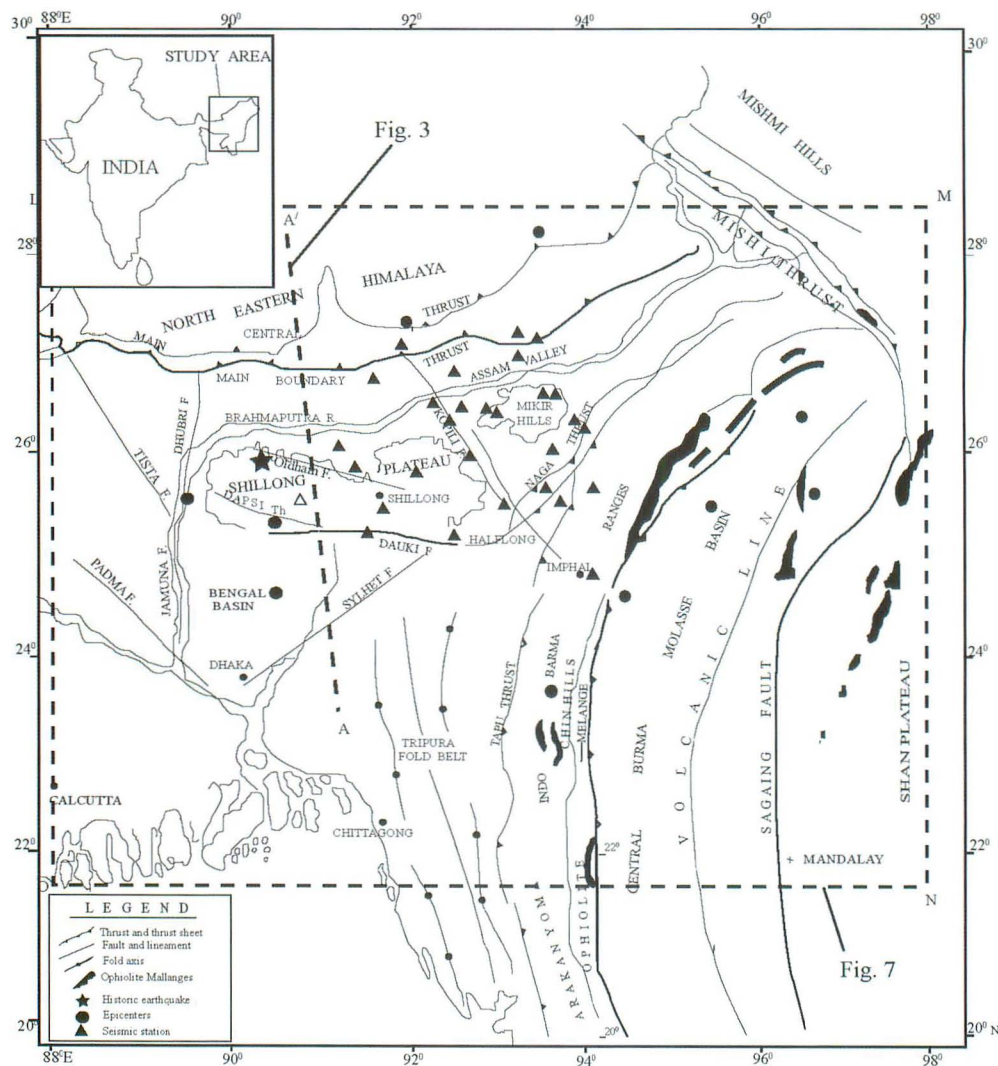


Fig. 1 Map showing major tectonic features in the study region (modified after Bhattacharya et al., 2008) and A-A' indicates the studied cross-section and dashed rectangle (LMNO) is area for plane stress study.

The orientation of tectonic stresses within the plate is related with the plate movement (Gowd et al., 1992) and varies within interplate and interior of the continent (Rajendran et al., 1992). The inter-relationship between orientation of stress and traction acting on a plate is well established when stress orientations are seen to be coherent over greater part of the plate (Gough et al., 1983). Rajendran et al. (1992) stated that intercontinental collision and convergent boundary produced enormous heterogeneous stress field over interplate region and stable part of the plate show similar distribution. No detailed studies yet have been conducted on stress distribution within the Bengal basin and adjacent regions, though there are some recent studies have been performed on geophysical exploration, focal mechanism solution, bore-hole break-out (e.g., Gowd et al., 1992; Rajendran et al., 1992 and Khan and Couhan, 1996, Gordon et al., 1999). For better understanding the stress orientation within the Bengal basin, Assam, the Indo-Burmese Range and its adjoining area, we try to assess the present-day tectonic condition under plane stress condition. The previous study of adjoining area (e.g., Gowd et al., 1992) and World Stress Map (WSM) are helping us to compare with our present study properly. The simulated result will help to reveal stress distribution, faulting pattern and displacement velocity of the study area. In this study we attempt to explain the significance of the Dauki and other major faults envisage regional stress pattern and their role on deformation velocity.

In the plane strain study, our approach is to simulate the present-day stress distribution and crustal deformation and examine the existence of Oldham fault along the northern boundary of Shillong Plateau. The geometry of Oldham fault proposed by Bilham and England (2001), is used for our models. Both the plane strain and plane stress modeling studies are performed by using FE software package developed by Hayashi (2008).

2. Geologic and tectonic setting

Collision tectonics formed by collision of Indian and Eurasian plates in the Southeast Asia (Chen and Molnar, 1990). The Bengal basin, the Shillong Plateau,

the Indo-Burmese Ranges and Assam region is one of the interesting places in term of seismicity, present-day crustal deformation caused by Indian lithosphere subsiding beneath the Burmese plate. The seismotectonics of the northeastern Bangladesh, the Shillong Plateau and Assam region is attributed to south directed overthrusting from the north due to collision of Himalaya and northward overthrusting at the Burmese Arc (e.g. Verma, 1976; Mukhopdhayay, 1988; Krisnan and Sanu, 2000, Kayal, 2001). Krisnan and Sanu (2000) also reports that the subduction trends of the Indian plate beneath the Burmese plate is $\sim N30^{\circ}E$ and deformation within the Burmese plate and its adjoining area is active accompanying with shallow earthquake events. Several studies have been done on plate reconstruction of the Indian subcontinent, and conclude that this area records the accretion of several plate and platelets of Gondwana. It is postulated that India rifted from combined Antarctica-Australia part of Gondwana-land and started its journey primarily north-westward and northward later in the Early Cretaceous (Alam et al., 2003). Alam et al. (2003) also cited that the continental Burma block also cut from Gondwana during Late Cretaceous to Paleogene. On the other hand, Khan et al. (1994) report that the Brahmaputra fault, Shillong Plateau and Yilgarn craton are acted as the major controlling factors for the distribution of Gondwana basins surrounding Assam and Bengal basin. The Bengal basin is considered as a remnant ocean basin at Early Miocene due to continuing oblique subduction of India beneath and southeast extrusion of Burma (Ingersoll et al., 1988; Alam et al., 2003). Khan and Agarwal (1993) described that the Bengal basin is within compression due to northeastern motion of the Indian plate and resistance offered by the Shillong Plateau that resulted in the development of differential movement within it. On the basis of recent frequent small earthquakes in these regions and recurrence of greater earthquakes indicate that the eastern and northeastern part of Bengal basin and Assam region are vulnerable for gigantic earthquake is predicted for near future (Islam, 2003).

3 Major geomorphic or tectonic features in the study area

Figure 1 shows the major geomorphic and tectonic elements in and around the study area. We describe major geomorphic subdivisions as follows-

3.1 Eastern Himalaya

The Himalaya is the largest orogenic belt in the world. An underthrusting of continental Indian crust and the entire Himalayan arc evolved as a consequence of collision of the Asian and Indian plate about 50 Ma (Angelier and Baruah, 2009). The Main Central Thrust (MCT) and Main Boundary Thrust (MBT) are the two major tectonic features in eastern Himalaya. The MCT is a major intercontinental ductile shear zone, which appears to have developed since mid-Tertiary time and also show minor recent activity. Two geologically distinct zones of Lesser Himalaya to the south and the Higher Himalaya Crystalline to the north, as separated by the MCT. The MBT is the main discontinuity between sub-Himalaya and Lesser Himalaya, presently characterized by intense disastrous earthquakes.

3.2 Sylhet trough

The Sylhet trough is an active subsiding basin of the Bengal basin in northeastern Bangladesh and is characterized by a large, closed, prominent negative gravity anomaly as low as -84 mgal (Alam, 1989). The Sylhet trough has minimal topography but huge sediments thickness ranges from about 13 to 17 km and of Neogene age (Johnson and Alam, 1991). The trough is separated by the Dauki fault from the Shillong Plateau, which is underlain by a basement complex of Archean gneiss, greenstone and late Proterozoic granite. The trough is bounded on the east and southeast by the sub-meridional trending folded belt of Assam and Tripura as the frontal deformation zone of Indo-Burman Ranges.

3.3 Bengal basin

Bengal basin is a remnant ocean basin at the beginning of Miocene (Alam et al., 2003) and consists of thick sedimentary cover (~13-18 km). The Jamuna-Dubri, the Meghna lineament is mentionable

with N-S trending faults or lineaments within the Bengal basin.

3.4 Shillong Plateau

Shillong Plateau is an average 1.0 km elevated structure in southeastern India and a part of Indian Shield, which is separated from Bengal basin by Dauki fault and by the Brahmaputra river valley from the Himalaya to the north. Shillong Plateau is a distinct landmass criss-crossed by numbers of faults and fractures in satellite image (Das et al., 1995) and consists of Precambrian gneiss, granitic, basalt (Sylhet traps) and Shillong group (sandstone and conglomerate) of rocks (Mishra and Shen, 2001). The Shillong Plateau occupies the area between the closely orthogonal thrust belts of the south-vergent the eastern Himalaya and the west-Indo-Burma micro plate and accommodates a considerable convergence within the area (Clark and Bilham, 2008). Abrupt rising of Shillong Plateau causes decrease and increase of seismic events within Bhutan and northeastern Bangladesh respectively (Bilham and England, 2001).

3.5 Dauki fault

Dauki fault is about 300 km long, wide and E-W trending the most prominent structural feature in the study area with steep scarps at some places especially in Bangladesh (Das et al., 1995. Hiller and Elahi (1984) suggested that Dauki fault is a south directed normal fault (cited in Das et al., 1995), whereas, Johnson and Alam (1991) state it as a north-directed low angle ($5-10^0$) thrust fault. According to Lohman (1995), this is high-angle reverse-fault at greater depth while right-lateral strike-slip faults near the surface but Alam et al. (2003) opined that the fault might be an upthrust fault.

3.6 Chittagong-Tripura folded belt

The eastern part of Bangladesh (Sylhet and Chittagong Divisions), Tripura, southern part of Assam, Mizoram and Myanmar territory are included in Chittagong-Tripura folded belt. Adjacent to S-E of the Chittagong hill tracts have a large number of narrow, elongated N-S trending folds with Tertiary sediments (Alam, 1989). These folds within Bangladesh is

characterized by ridge forming, box-like in cross section, high amplitude with variable width and lie en-echelon with the adjacent structures. Some of the structures are faulted and thrust, and the intensity of folding increases gradually from west to east.

3.7 Assam and Brahmaputra valley

Assam region is characterized by folded and faulted with huge sediments thickness (~ 13 km) as observed within the Bengal basin. Major tectonic elements of the region are Mikir hills, Disang thrust, Naga thrust, Kopilli lineament and the Brahmaputra lineament (Fig. 1). This region is bounded by the MBT to the north and its south is Shillong Plateau. The Brahmaputra valley is an ENE-WSW trending narrow valley bounded by Mishmi block to the northeast, the Himalayas to the north and by the Shillong Plateau to the south. This valley is covered by 3-4 km thick sediments. The NE striking the MBT was ruptured by a major earthquake (M 8.7) in 1950 and associated with thrust faulting along shallow north dipping plane (Gowd et al., 1992).

3.8 Indo-Burmese Ranges

The western edge of the Indo-Burmese range is bounded by thrust faults along the Naga hills in the north. Folds and thrusts are same orientation as found eastern part of the Bengal basin. Field investigations suggested that this area consists of Tertiary to Quaternary sediments (Evans, 1964; Curray and Moore, 1974; Chen and Molnar, 1990). The eastward dipping seismic zone under the Indo-Burmese range indicates that the Indian lithosphere was underthrust beneath this region (Chen and Molnar, 1990). They also inferred that the Indian plate has been flexed down considerably during subduction period under Indo-Burmese ranges.

4 Geodynamics of the Study area

An underthrusting of the eastern Indian plate under the Eurasian plate form a complex deformation regime (Jade et al., 2007). The Shillong Plateau is currently behaving like a rigid body that is coupled to the Indian plate and moves at 46.5 ± 1 mm/yr in a direction $N51^\circ E$ (Jade et al., 2007). The previous studies (e.g., Chen et

al., 2000; Shen et al., 2000; Holt et al., 2000; Paul et al., 2001; Sella et al., 2002; Socquet et al., 2006; Jade et al., 2007; Malaimani et al., 2000) report that the velocity of Indian plate relative to the Eurasia plate is between 34.8 to 43.7 mm/yr, which is lower than NUVEL-1A modeling (45 mm/yr) of De Mets et al. (1994). Furthermore Krishna and Sanu (2000) report a N-S compressional deformation of 18.9 ± 2.5 mm/yr, an E-W extension of 17.1 ± 2.2 mm/yr and a vertical component of the velocity tensor 2.4 ± 0.3 mm/yr in the Shillong Plateau. They also show that the compressional velocity is 5.4 ± 2.8 mm/yr along $N33^\circ E$ in the Bengal basin and Tura folded belt in the Shillong Plateau. Biswas et al. (2007) show that the Sylhet trough is subsiding at the value at 0.45 mm/yr, whereas the Shillong Plateau and the Assam- Brahmaputra valley are uplifting at a rate of 0.32-0.80 mm/yr and 0.12-0.67 mm/yr respectively. Northward movement of the Indian plate is the main cause of crustal deformation within the Shillong Plateau and its adjoining areas. Pop up or vertical uplift of the Shillong Plateau has also been considered as an agent for the cause of deformation, though its contribution is <2% if the rapid uplift rates of 10 mm/yr (Holt et al., 2000).

Krishna and Sanu (2007) report that the Bengal basin and Tripura folded belt assumed to be have compression of 5.4 ± 2.8 mm/yr along $N33^\circ E$. Jade et al. (2007) reported from GPS measurement that the Shillong Plateau moves average 33.5 ± 0.4 mm/yr toward NE with the Eurasian reference plate where as the Indo-Burmese belt has velocity ~ 30 mm/yr. Krishna and Sanu (2007) also show that northern part of the Sagaing transform fault deforming both with extension of 29.5 ± 4.7 mm/yr and with compression of 12.4 ± 1.9 mm/yr along $N74^\circ$ where as southern part also show a compression of 17.4 ± 2.3 mm/yr and 59.8 ± 8.0 mm/yr extension along $N71^\circ$. During 1997-1999, GPS measurement indicates that the active convergence is 6.3 ± 3.8 mm/yr (Paul et al., 2001) between the central Shillong Plateau and the point in central and southeast India. Presentt studies (e.g., Bilham and England, 2001; Jade et al., 2004) on GPS velocity infer that probably ~30% of the 15-19 mm/yr convergence across the eastern Himalayan system accommodated the Shillong Plateau (Clark and Bilham, 2008). Clark and Bilham

(2008) also suggest that deformation of the Shillong Plateau indicates differentiation of the eastern Himalayan from rest of the Himalaya and significant change in regional strain partitioning. Moreover Angeiler and Baruah (2009) showed that the displacement velocity of the Shillong Plateau and

Bengal basin is similar with respect to Eurasia, but Shillong Plateau show slower (~50%) velocity with respect to Lhasa in GPS study (Fig 2). This statement is contradictory that indicate northeastern part of Indian plate subject to aseismic creep with in temporary locked situation.

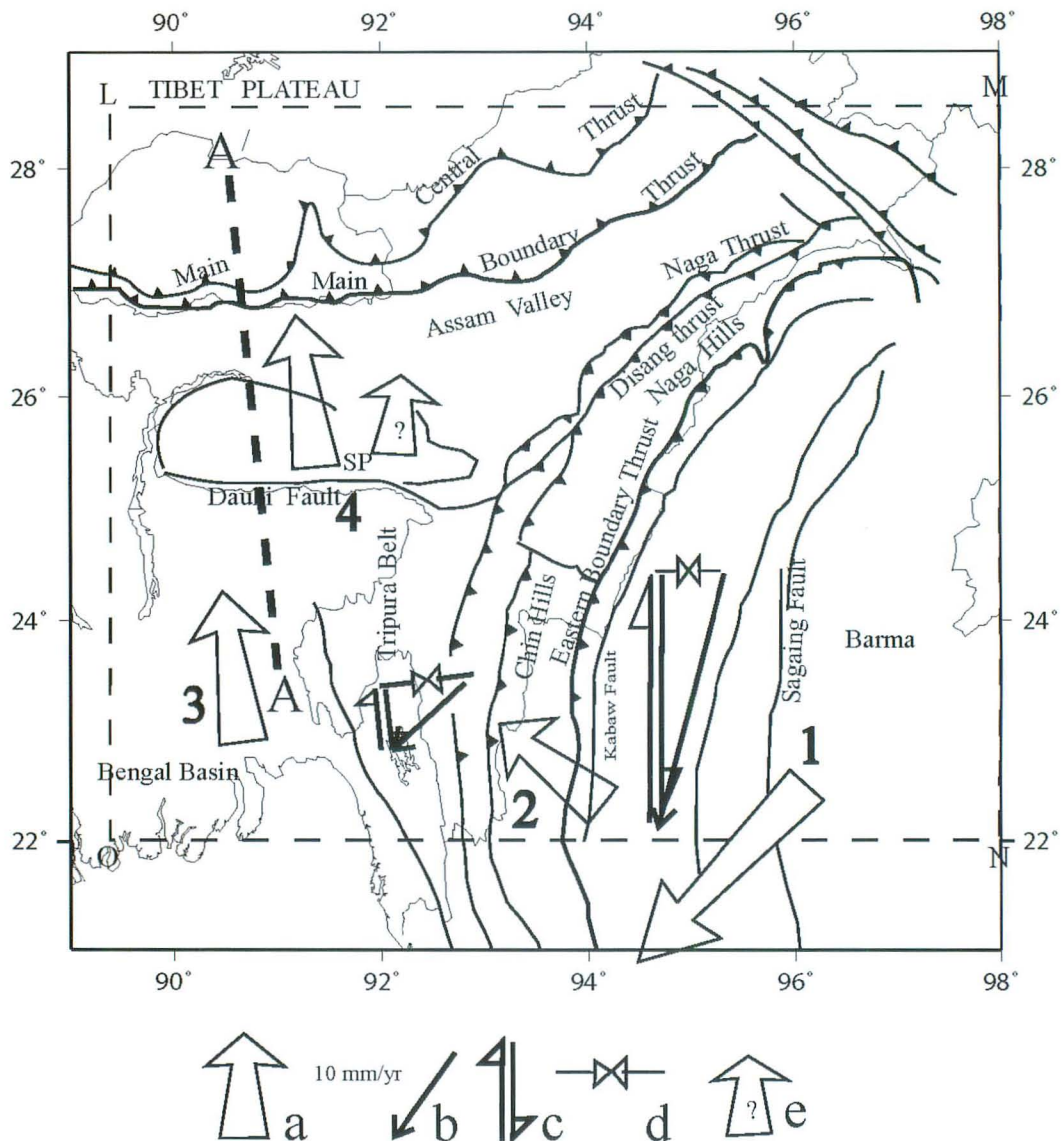


Fig. 2 Geodynamic setting of the study area (modified after Angeiler and Baruah, 2009).

Clark and Bilham (2008) also report focal mechanism and gravity data suggest the existence of thrust fault beneath the Shillong Plateau but sense of motion of the Dauki fault has not been clear. Ray et al. (2005) reported that Rajmahal-Bengal-Sylhet igneous province experienced widespread and rapid emplacement of tholeiitic basalt flow ($\sim 118 \pm 2$ Ma) and such large volcanism is directly related to Kerguelen

plume of Australia. Sylhet-Bengal-Rajmahal traps also indicative to mantle plume that supports Bilham and England's (2001) 'pop up' modeling. This tholeiitic basalt flow of the Rajmahal-Bengal-Sylhet Traps of eastern India is the part of large igneous provinces and is considered to be represents volcanic filled (Kent et al., 2002).

5 Modeling

Stress condition within the Earth depends on the rheology of a particular region. In the plane strain study, a suitable geological cross-section should be selected to estimate the stress condition and convergence induced deformation within the elastic continuum. We selected the geologic cross-section (Fig. 3) of Bilham and England (2001) for finite element modeling. The entire

cross-section area for plane strain and a morphotectonic map (Fig. 4) of Bhattacharya et al. (2008) were selected for plane stress and were divided into small triangular elements or domains. A mesh is generated with 2242 elements and 1200 nodes for both cases. Simulation is performed using FE software package developed by Hayashi (2008).

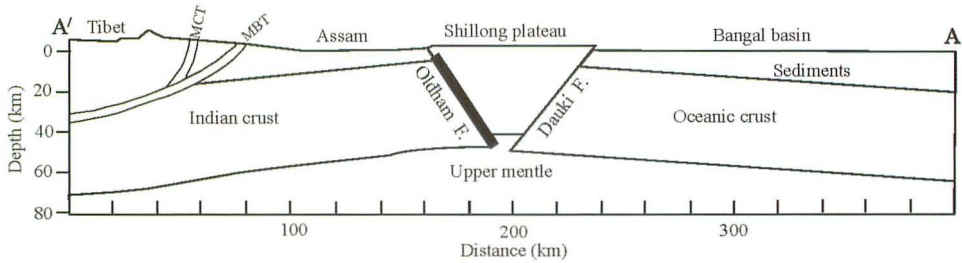


Fig. 3 North-south cross-section (A-A' shown in Fig. 1) from Tibet to the Bay of Bengal showing schematic 'pop-up' geometry of SP (simplified from Bilham and England, 2001).

5.1 Plane strain case (I)

5.1.1 Model set up

About 400 km long and 80 km deep selected section lies along the longitude 91°E. Twelve layers (Table 1) are considered within the model (Fig. 4). The Tertiary-Recent deposits in the upper crust in the Assam valley (layer 7) and in the Bengal Basin (layer 12) are considered as a single lithologic unit (Table 1). The lower crust under Assam region is Indian crust (Layer 2) consisting of granite, syenite, basic and ultrabasic rocks (Santosh, 1999), while the lower crust beneath the Bengal basin is considered oceanic crust

(Layer 11). The oceanic crust mainly consists of tholeiitic basalt, gabbro, rhyolite, migmatite, diatexite, granulite, mylonite and other basaltic rocks. We also consider the upper mantle (down to 84 km depth) as one lithologic unit (Layer 1). According to Keary and Frederick (1998), upper mantle is to be formed by peridotite, dunite, gabbro, eclogite and other olivine-rich rock. We consider MBT, MCT, Oldham fault and Dauki fault as a separate rock layer (Layer 3, 4, 8 and 10 respectively) as sheared weak rocks. We also taken into account the rheology for Tibetan Himalaya and Lesser Himalaya (please see in table 2).

Table 1 Rock layer property in plane strain models.

layer	Density (kg/m ³)	Young's modulus (GPa)	cohesion (MPa)	internal friction angle (degree)	references
1	3300	110	19	46	Khan and Hoque, 2006; Rajeskhar and Mishra, 2008; Clark, 1966 and this study
2	2900	100	18	55	
3	2000	1	14	42	
4	2000	1	14	42	
5	2600	65	16	46	
6	2450	60	15	55	
7	2400	50	16	42	
8	2000	1	14	42	
9	2800	80	18	55	
10	2000	1	14	42	
11	2850	85	18	55	
12	2400	50	17	55	

Poisson's ratio is 0.25.

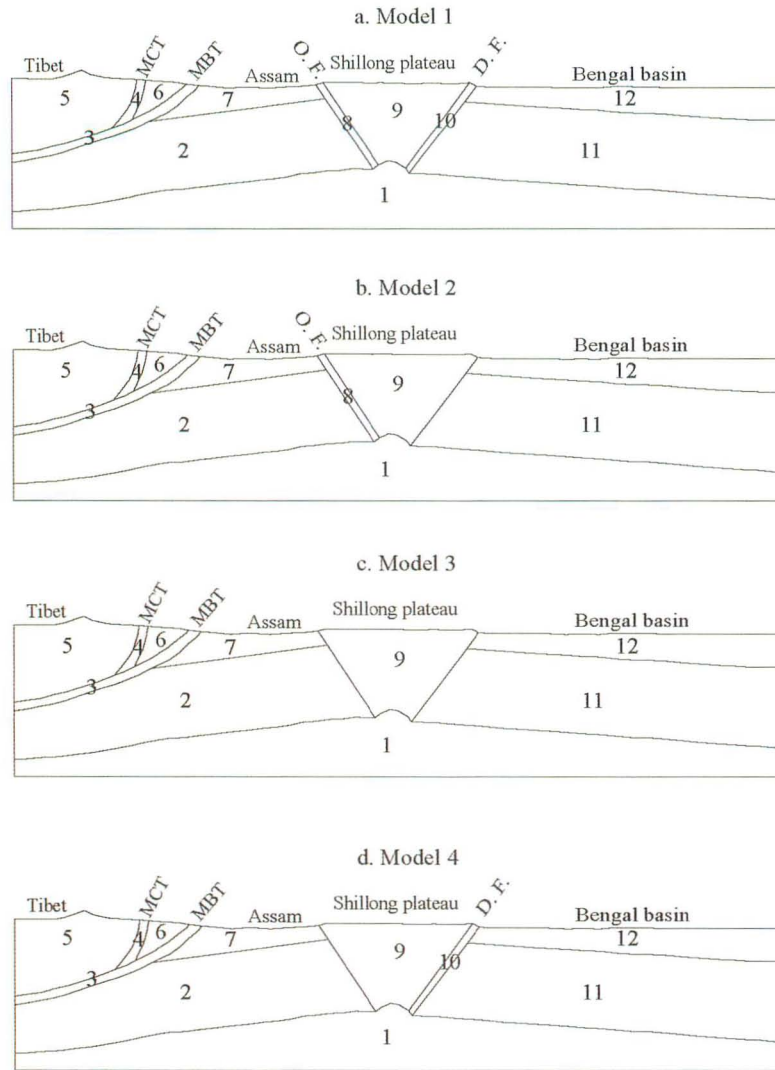


Fig. 4 Models in study (a) model 1, (a) model 2, (c) model 3 and (d) model 4.

Four geometric models have been examined. In the model 1 (Fig. 4a), twelve layers are considered as mentioned above. The model 2, consists all the layers of model 1 except the Dauki fault (Fig. 4b). In the model 3, we remove both the two fault zones (Fig. 4c) and in the model 4, we remove the Oldham fault (Fig. 4d).

5.1.2 Boundary condition

The boundary conditions applied to the model (model 1) shown in Fig. 5 is assumed 200m convergence between Indian plate and Eurasian plate. Two boundary conditions (BC 1 and BC 2) are constructed on the basis of vertical uplift. Both boundary conditions are shown in Fig.5. In the model with the BC-1 (Fig. 5a), horizontal displacement of 200

m at the rate 46.5 ± 1 mm/yr of the Indian plate for $\sim 4,283$ yrs, (Jade et al., 2007) has been applied along x-axis from right to left with fixed vertical dimension, and the displacement gradually decreases toward left and becomes zero at the rear nodal point. All nodal points in right side of the model have equivalent displacement. We fixed rear nodal point at the bottom end of the left side and free slip boundary condition has been used along left wall of the model. The left side is fixed in horizontal dimension and free along y-axis. The upper part of the model is kept for free movement, and it represents the Earth surface. Vertical displacement of 1.3-3.4 m at the rate of 0.3-0.8 mm/yr for $\sim 4,283$ yrs, (Biswas et al., 2007) has been applied from the bottom end of the model with the BC-2 (Fig. 5b).

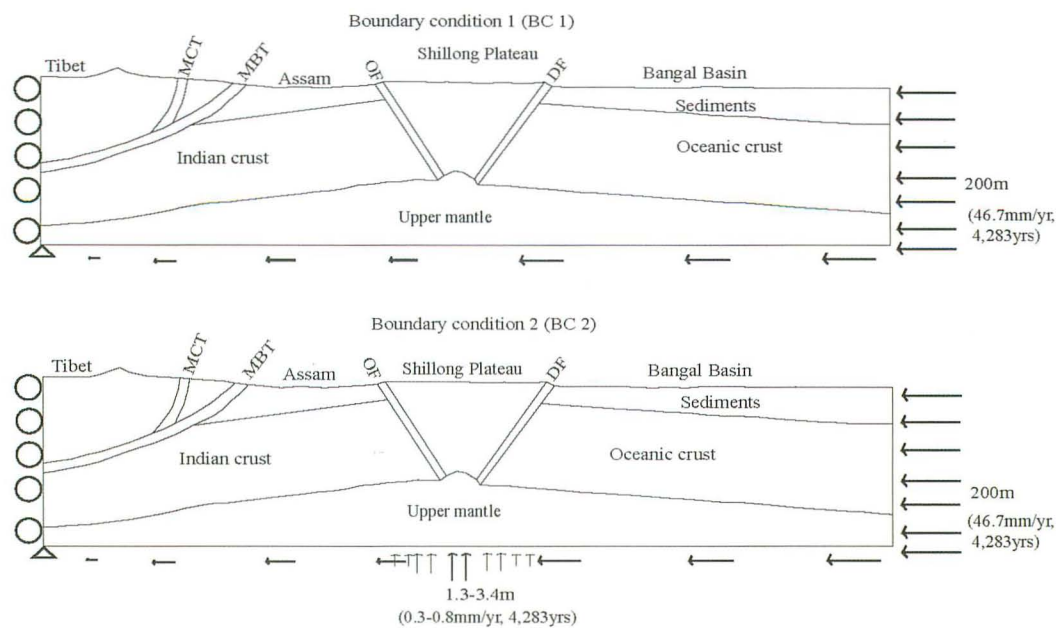


Fig. 5 (a) Boundary condition 1 and (b) Boundary condition 2.

5.1.3 Rock layer property

The rock layer properties influence the results of numerical modeling and as well as the state of stress within the model. Crustal structure and earthquake focal depths in the Shillong Plateau and adjoining areas provide significant information on the rheology of continental crust. It is observed that most of the earthquakes occur within the lower crust at 15- 30 km (Kayal and De, 1991; Kayal, 2001; Kayal et al., 2006). Chen and Molnar (1990) suggested that a few earthquakes are even deeper down to 50 km in the Shillong Plateau. Macwell et al. (1998) reported that change in mineralogy across the Moho, the olivine-rich

uppermost mantle rock, also shows strong brittle regime due to dry condition.

Rock properties such as density, Young's modulus, Poisson's ratio, angle of internal friction and cohesion used in the model are shown in Fig.6 and Table 2. The density values are taken from Rajeskhara and Mishra (2008) and Khan and Hoque (2006). The average density values range between 2000 kg/m³ (for layer 3, 4, 8 and 10) and 3300 kg/m³ (for layer 1) in the model 1 (Fig. 4a). The values of Young's modulus, cohesion and angle of internal are taken from Clark (1966), and we used 0.25 as Poisson's ratio.

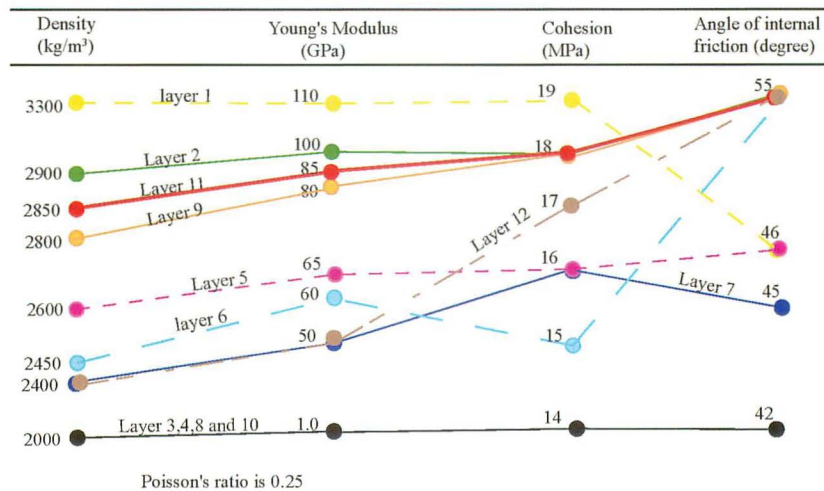


Fig. 6 Rock layer property for plane strain models.

Table 2 Layers of the rock unit used in plane strain models.

layer	major unit	rock type	reference
Layer 1	Upprer Mantle (Depth down to 84 km)	Peridotite, dunite, kimbertite pyrolite, gabbro, eclogite etc.	Keary and Frederick, 1998
Layer 2	Indian Crust	Granite, Syenite, basic and ultra-basic rocks	Santosh, 1999
Layer 3	MCT	Weak rheology	this study
Layer 4	MBT	Weak rheology	this study
Layer 5	Higher Himalaya	Gneiss and granite	Hodges, 2000
Layer 6	Lesser Himalaya	Siwalik sediments with limestone and metasediments	Hodges, 2000
Layer 7	Sedimentary unit within Assam valley	Tertiary-Recent Sandstone, siltstone, limestone and loose sediments	Evans, 1964; Kent and Dasgupta, 2004
Layer 8	Oldham fault zone	Weak rheology	this study
Layer 9	Shillong Plateau	Archean gneissic complex, schist, ultramafic alkaline carbonate, metasedimentary Shillong Group and Cretaceous-Tertiary sediments	Evans, 1964; Mishra and Sen, 2001
Layer 10	Dauki fault zone	Weak rheology	this study
Layer 11	Oceanic crust below Bengal basin	Tholeiitic basalt, Gabbro, rhyolite, migmatite, diatexite, granulite, mylonite and other basaltic rocks	Brown and Rushmer, 2006
Layer 12	Sedimentary unit within Bengal basin	Tertiary-Recent deposits of Sandstone, siltstone, limestone and loose sediments.	Johnson and Alam, 1991; Alam et al., 2003

5.2 Plane stress case (II)

5.2.1 Model set up

The models are constructed by taking the simple morphotectonic map (Fig. 7). The entire area is 775 km \times 1000 km and lays longitude between 89° E and 98°E and latitude between 20°N to 30°N. The total area is divided into small triangular elements or domains. A mesh is generated with 1682 elements and 900 nodes within the area. We divide the entire study area into 6 zones (Fig. 8) on the basis of rock property (Table 3). The two dimensional horizontal area is represented by finite element model. All faults (the Dauki fault, the Meghna fault, the Jamuna-Brahmaputra fault, the MBT, the Kopilli fault, the Arakan Yoma suture zone and the

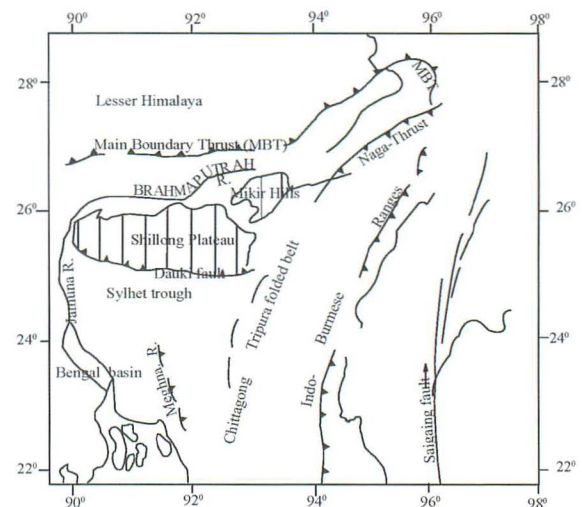


Fig. 7 Morphotectonic map of the study area (Modified after Bhattacharya et al., 2008).

Sagaing fault) have been considered as a zone with weak rheology. And others zones are (a) the Bengal basin including Sylhet trough (b) the Shillong Plateau (c) the Brahmaputra valley (d) the Himalayan front and (e) the Indo-Burmese zone including Chittagong-Tripura folded belt. The Bengal basin (including Sylhet trough) and the Brahmaputra valley consists of thick sedimentary cover of the Quaternary

to recent age (Alam et al., 2003). The Shillong Plateau consists of Archean gneissic complex, metasedimentary Shillong Group rocks, igneous rocks, porphyritic granites, alkaline-carbonate complexes and Cretaceous-Tertiary sediments (Biswas and Grasemen, 2005). The rock of the Indo-Burmese Range and Chittagong-Tripura folded belt is composed of Tertiary sediment (Alam, 1989).

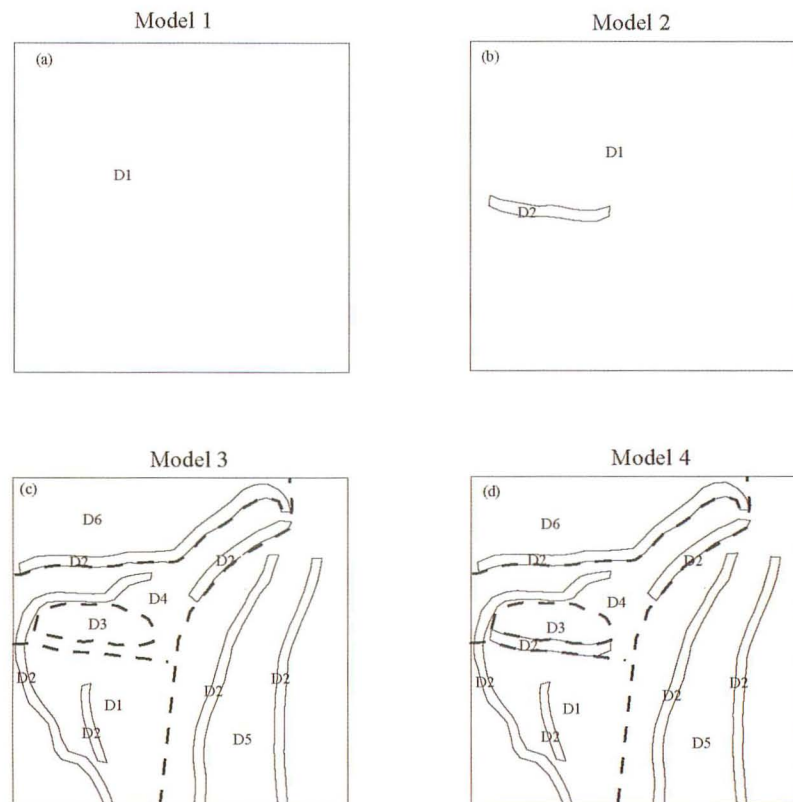


Fig. 8 Geometry of the models with layers (a) model 1, (b) model 2, (c) model 3 and (d) model 4.

Four different geometric models have been constructed on the zones considered in the modeling and is shown in Fig. 8. All for models are based on the presence or absence of the Dauki fault. We choose

uniform lithology for entire model area, whereas, Dauki fault is assumed within model 2. In model 4, all fault zones are selected within the model while we remove the Dauki fault within model 3.

Table 3 Layer of the rock used in the plane stress models.

layer	major unit	rock type	reference
Layer 1	Bengal basin	Tertiary-Recent deposits of Sandstone, siltstone, limestone and loose sediments.	Johnson and Alam, 1991; Alam et al., 2003
Layer 2	fault zones	Weak rheology	in the study
Layer 3	Shillong Plateau	Archean gneissic complex, schist, ultramafic alkaline carbonate, metasedimentary Shillong Group and Cretaceous-Tertiary sediments	Evans, 1964; Mishra and Sen, 2001
Layer 4	Assam valley	Tertiary-Recent Sandstone, siltstone, limestone and loose sediments	Evans, 1964; Kent and Dasgupta, 2004
Layer 5	Chittagong-Tripura folded belt and Indo-Burmese Range	Neogene sediments, basic and ultra-basic mafic rocks, ophiolites, Paleozoic sediments and metamorphic rocks	Acharyya, 2007 Evans, 1964
Layer 6	Himalayan Front	Siwalik sediments, Piedmond deposits, sandstone and siltstone with Recent sediments	Yeats and Thakur, 2008

5.2.2 Boundary Condition

Northward movement of the Indian plate is the driving force of crustal deformation within the study area has been chosen in the boundary conditions (BC). The boundary conditions that applied in models are shown in Fig. 9. In the models, 46.5 ± 1 mm/yr horizontal velocity of the Indian plate (Jade et al., 2007) with Eurasian reference in the direction of $N90^\circ E$ and $N51^\circ E$ has been applied. A 1000m convergent displacement for 21,412 yrs is assumed between the Indian plate and the Eurasian plate. In BC 1 and 2 (Fig. 9(a-b)), we propose northward and angular horizontal displacement of Indian plate from

south. Eastern and western portion of the model used to keep free for movement. Northward uniform velocity imposed from the southern boundary of the model, and eastward displacement (gradually decrease toward north) from western boundary in BC 3 (Fig. 9(c)). In fourth boundary condition (Fig. 9(d)), we also chose same boundary displacement as boundary condition 3 but with angular velocity. We propose differential surface movement within the model in BC 5 and illustrated in Fig. 9(e). Moreover, we consider active plume or rifting along the Dauki fault in this boundary condition. The BC 6 almost similar with BC 4, but we fixed the Dauki fault for further movement (Fig. 9(f)).

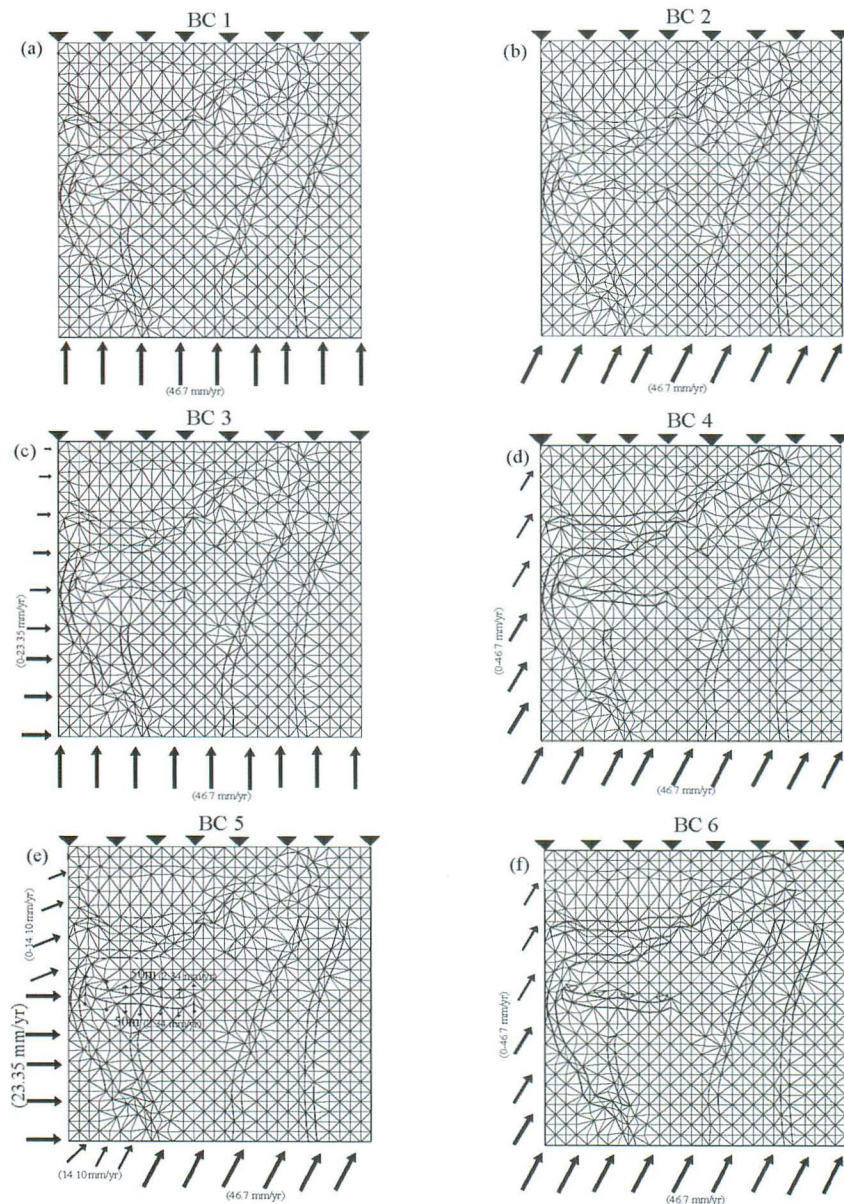


Fig. 9 Boundary Condition of the models. (a) BC 1, (b) BC 2, (c) BC 3, (d) BC 4, (e) BC 5 and (f) BC 6.

5.2.3 Rock layer property

Numerical modeling results as well as state of stress within the model largely depend on rock layer property. The earthquake focal depth studies and crustal structure of the study area have significant influence on the rheology. We consider that the total area is behaving elastic brittle materials over geologic time span with homogeneous rheology. Major rock domain properties such as density, Young’s modulus, Poisson’s

ratio, internal angle of friction and cohesion are used in the modeling which is shown in Table 4 and Fig. 10. The density values are taken from Rajeskhar and Mishra (2007), Khan and Hoque (2006) and Verma and Mukhapadya (1977). The values of Young’s modulus, cohesion and angle of internal friction have been chosen from Clark (1966) and we use 0.25 as the standard value of the Poisson’s ratio in the model calculation.

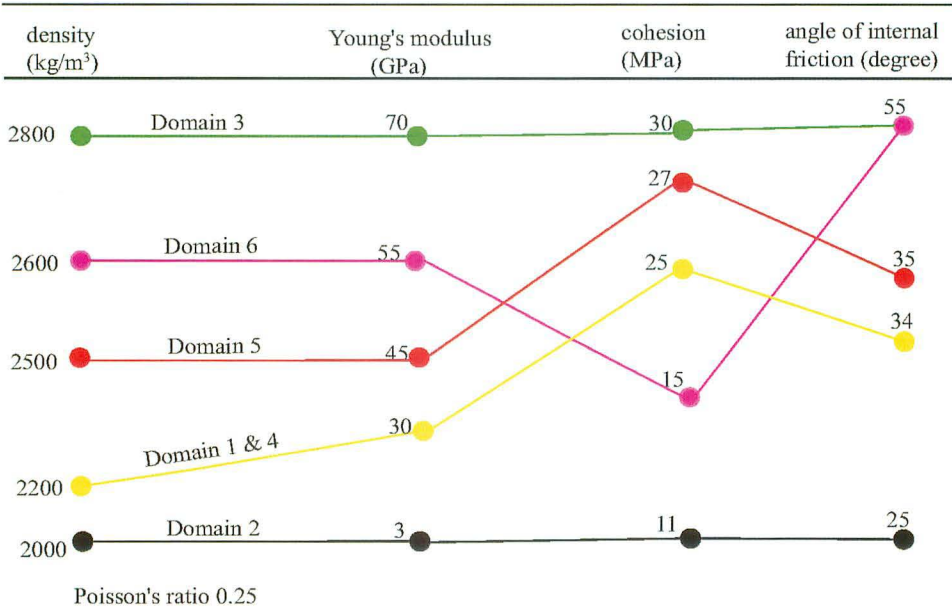


Fig. 10 Rock layer property for plane stress models

Table 4 Rock layer property in plane stress models.

Layer/major rock unit	density	Young's modulus (GPa)	cohesion (MPa)	internal friction angle (degree)	references
Bengal basin	2200	30.0	25	34.0	Khan and Hoque, 2006; Rajeskhar and Mishra, 2008; Clark, 1966 and this study
fault zones	2000	3.0	11	25.0	
Shillong Plateau	2800	70.0	30	55.0	
Assam valley	2200	30.0	25	34.0	
Chittagong-Tripura folded belt and Indo-Burmese Range	2500	45.0	27	35.0	
Eastern Himalaya	2600	55.0	15	55.0	

Poisson's ratio 0.25

6 Results

6.1 Result of plane strain case (I)

The spatial distribution and orientation of the stress are obtained at each node of the mesh. The calculated stress fields and faulting patterns show the significant changes in relation to the applied convergent displacement within the model. A series of model calculations have been carried out, but only the representative models are described here. We impose horizontal convergent displacement of 50, 200 and

1000 m with vertical uplift of 10, 40 and 200 m respectively to the boundary condition at BC-2, and only horizontal displacement is applied to the boundary condition at BC-1. The modeling results presented here are based on: (i) stress distribution, and (ii) distribution of failure element.

6.1.1 Stress distribution

Figure 11 represents the simulated spatial distribution pattern of principal stresses of 200 m

convergent displacement for model 1, 2, 3 and 4 using boundary condition of BC 1. The maximum compressive stress (σ_1) and minimum compressive stress (σ_3) are aligned vertically and horizontally in the Bengal basin and Assam valley in all the models, except the area close to the faults. However, considerable changes are observed in stress orientation pattern within the deeper part of the models near the Dauki fault, bottom of the Shillong Plateau and near the Oldham fault, which are the prominent areas of stress accumulation in the study region (Fig. 11). Within the fault zones, the orientation of σ_1 is normal to the fault, where stress magnitude is smaller than that of the adjoining areas. This indicates that a considerable convergent displacement is accommodated within these fault zones. We can find complex stress distribution exists beneath the SP in model 1 (Fig. 11a). The upper part of the Shillong Plateau shows tensional stress, whereas the deeper part shows change in compressional

stress. In model 2, the upper part of the Bengal basin and the Shillong Plateau show distinct changes in orientation of principal stresses (Fig. 11b). It also illustrates that the tensional stress is restricted within shallow depth in the Shillong Plateau, and it propagates to the upper part of the Bengal basin. This stress change is simulated in the model without the Dauki fault. The stress distribution is unchanged in other areas of the model 2. In the model 3, the entire region shows compressive stress regime, and tensional stress regime is absent. The Shillong Plateau shows little change of principal stress orientation though both the Dauki and Oldham faults are absent in the model (Fig. 11c). The upper part of the Shillong Plateau and Assam valley in model 4, tensional stress is dominated (Fig. 11d). Deeper part, near the Dauki fault and bottom of the Shillong Plateau, shows unchanged stress distribution. The model 4 shows a similar trend of stress orientation as in model 1.

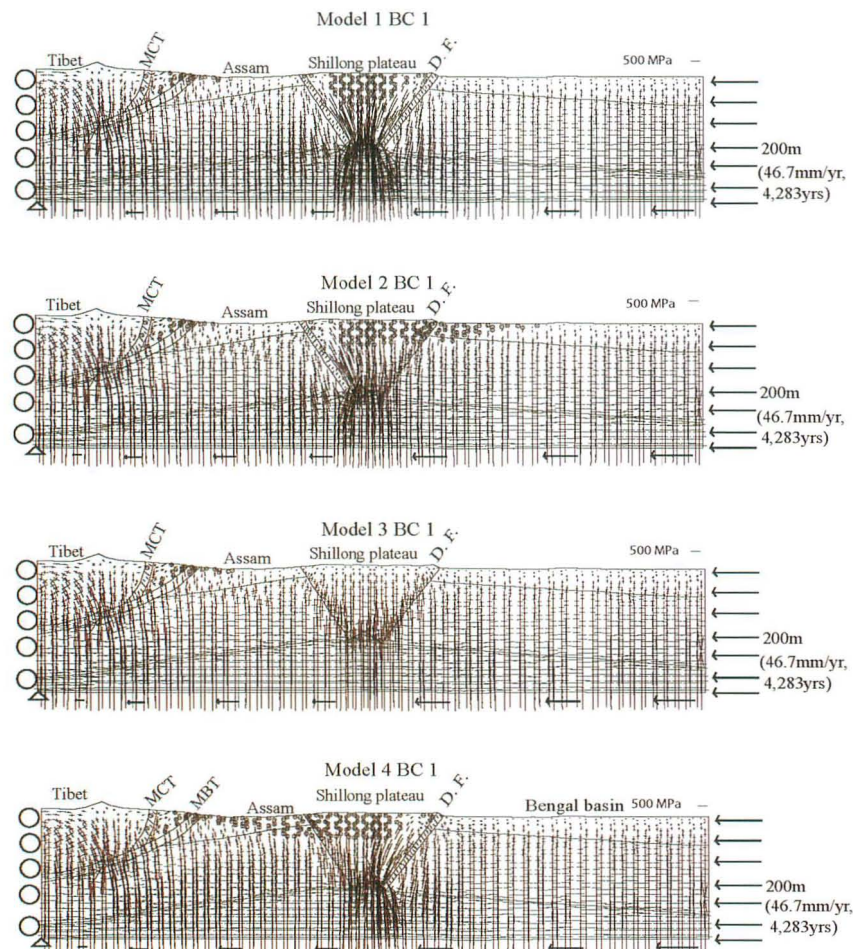


Fig. 11 Distribution of principal stresses of model 4 under BC-1 at (a) 50m, (b) 200m and (c) 1000m convergent displacement. Circle represents tension stress.

Almost similar type of stress distribution is observed modeling using boundary condition BC-2, except the areas close to the upward displacement (Fig.

12). With increasing convergent displacement, the model shows progressive increase in compressive stress regime and orientation of σ_1 and σ_3 rotate anticlockwise

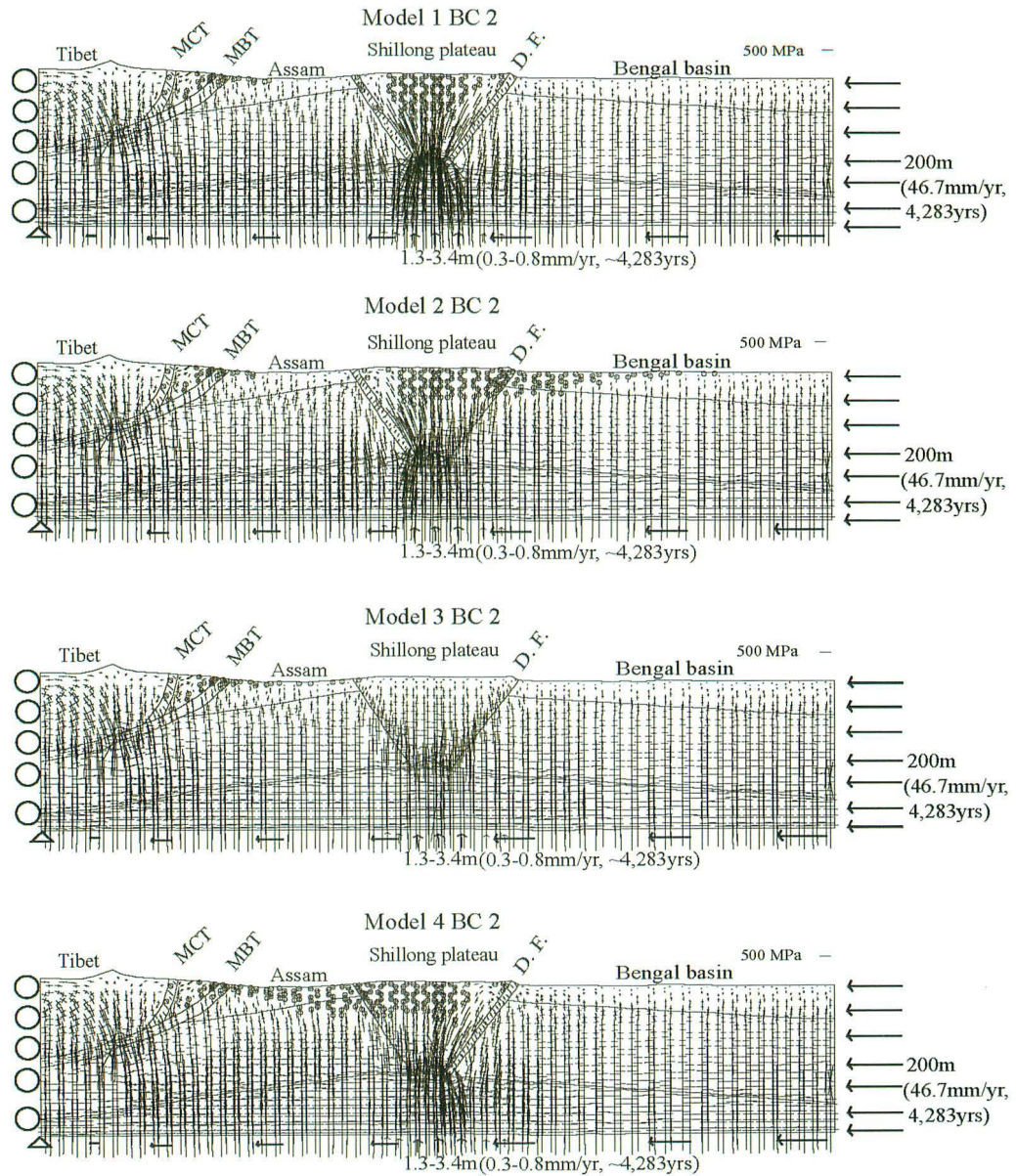


Fig. 12 Distribution of principal stresses under BC-2 at 200m convergent displacement for (a) model 1, (a) model 2, (c) model 3 and (d) model 4. Circle represents tension stress.

adjoining the Shillong Plateau and at the fault zones (Fig. 13). In greater convergent displacement (model 4, BC-1, 1000 m) the rotation of principal stresses increases from shallow to deeper part in the Assam valley (Fig. 13c), and the tensional stress regime reduces significantly. The characteristic changes in orientation of principal stresses (vertical to horizontal) are an excellent indicator of thrust faulting in convergent tectonic environment. Non-uniform stress is

distributed in the model 4 using boundary condition BC-1 shown in Fig. 14. The simulated shear stress indicates that its significant maximum value lies almost at the bottom of the Shillong Plateau crust and the Dauki fault zone. This result is important for the study area, because it implies that the areas of higher shear continuously accumulate considerable amount of stress within the Shillong Plateau between the interseismic periods.

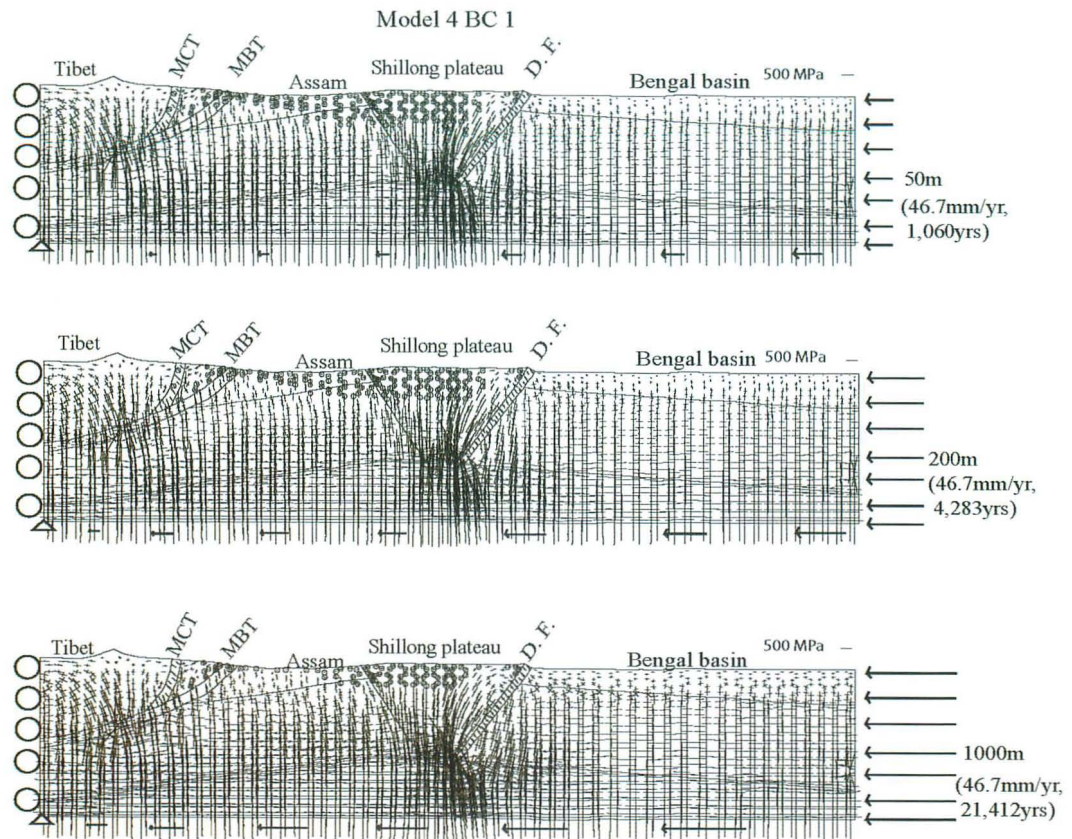


Fig. 13 Distribution of principal stresses under BC-1 at 200 m convergent displacement for (a) model 1, (a) model 2, (c) model 3 and (d) model 4. Circle represents tension stress.

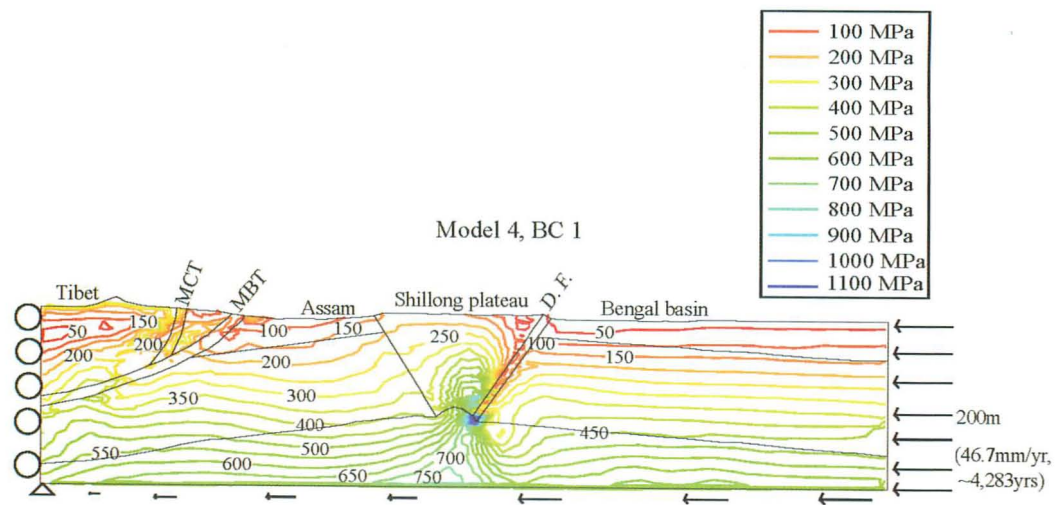


Fig. 14 Contour of maximum shear stress in the SP, Assam and the Bengal Basin for model 4 under BC-1 at 200m convergent displacement.

6.1.2 Distribution of failure element

Our simulated results show the existence of both interseismic deformation and fault development in the study area. The Mohr-Coulomb failure criterion is used to analyze the fault development in the FE software package (Hayashi, 2008). Fig. 15(a-d) shows the computed principal stresses within failure elements of

four models (model 1-4). All models show different pattern of fault development under BC 1. It is find that the failure elements that both the Dauki fault and the Oldham fault are of thrust faulting zones, but upper part of the Shillong Plateau shows normal faulting environment in model 1 (Fig. 15a). Model 2 (Fig. 15b) also shows presence of thrust faulting within the

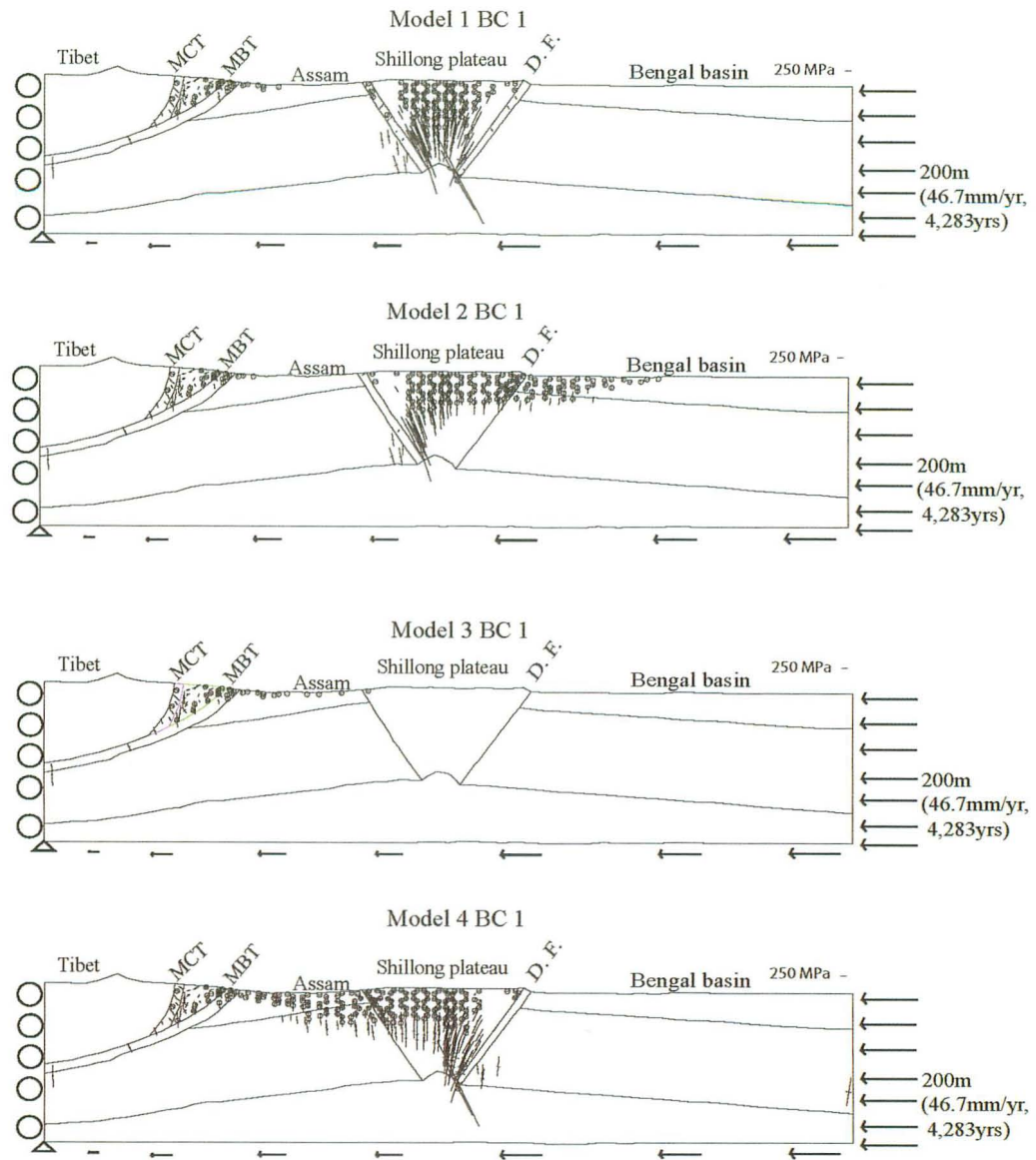


Fig. 15 Principal stress within failure elements of the models for BC-1 under 200m convergent displacement for (a) model 1, (a) model 2, (c) model 3 and (d) model 4. Circle represents tension stress.

Oldham fault zone, but there are normal faulting in the Bengal basin and in the upper part of the Shillong Plateau. This may be the result due to absence of the Dauki fault in this model. Fig. 15c does not show any failure, and it could be due to the absence of both the Dauki and Oldham faults in the model 3. The Shillong Plateau and Assam valley show significant normal faulting and the Dauki fault shows thrust faulting in model 4 (Fig. 15d). Same pattern of fault distribution is also observed in models under BC-2 (Fig.16). Model 4 under BC 1 is the best fit model which simulates a realistic and natural faulting and failure elements in the Shillong Plateau, Assam and the Dauki fault zone,

though this model does not show significant failure in the Bengal basin. In progressive convergent displacement (Fig. 17a-c), especially in case of 1000 m displacement (Fig. 17c), the tensional failures are reduced significantly and restricted within the Shillong Plateau and its surrounding areas. The fault zones show similar faulting pattern as seen in lesser convergent displacement.

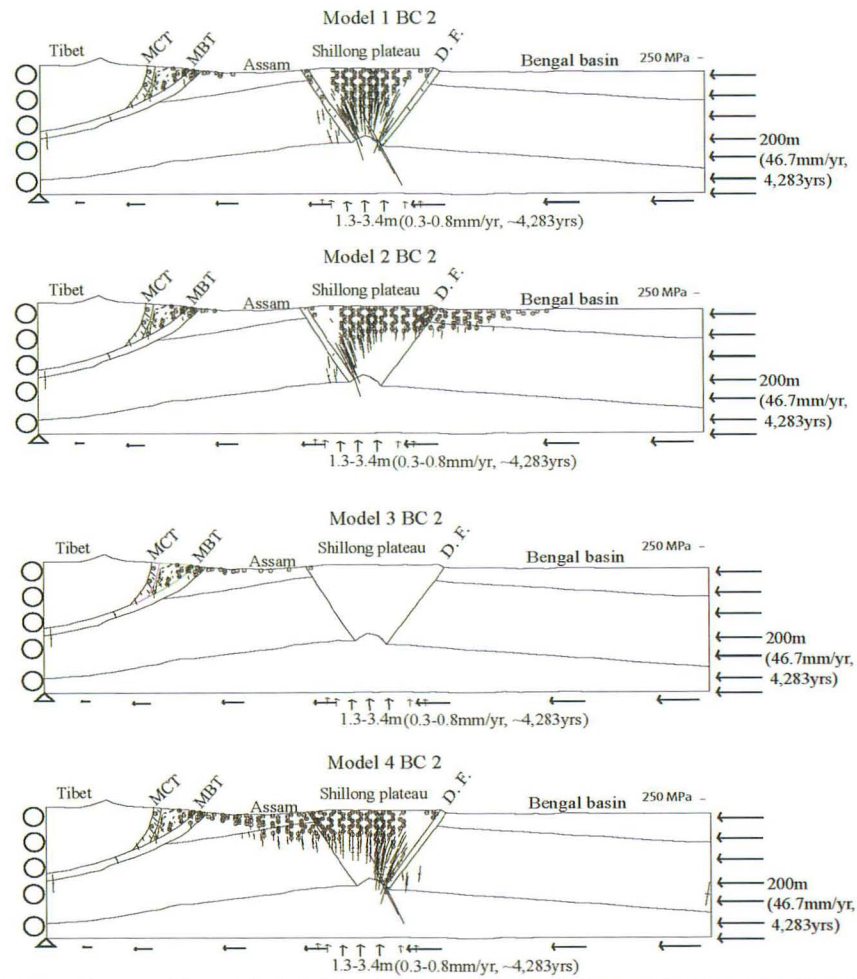


Fig. 16 Principal stress within failure elements of the models for BC-2 under 200m convergent displacement for (a) model 1, (a) model 2, (c) model 3 and (d) model 4. Circle represents tension stress.

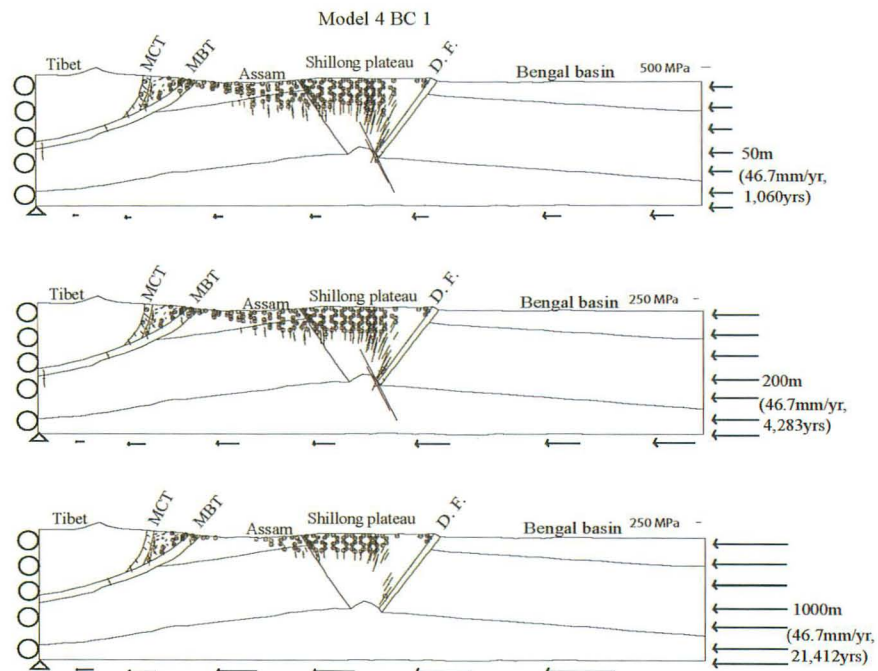


Fig. 17 Principal stress within failure elements of the model 4 under BC-1 for (a) 50m, (b) 200m and (c) 1000m convergent displacement. Circle represents tension stress.

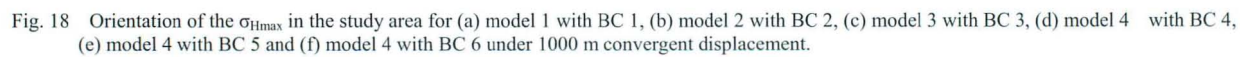
6.2 Result of plane stress case (II)

We simulate the pattern of stress field under different convergent boundary conditions. State of stress is one of the useful techniques to understand the proximities of the ongoing crustal deformation and neotectonics which depend mainly on imposed boundary conditions, model geometry and rock rheology. The Himalyan front, the Dauki fault, the Shillong Plateau, the Bengal basin and the Indo-Burmese Ranges are the major morphotectonic unit and among these, the Dauki fault is the most prominent southern boundary fault of the Shillong Plateau which is playing important role on the deformation in the study area and controls the contemporary stress field as well. The spatial distribution and orientation of stresses are obtained at each node of the mesh. The calculated stress field, faulting pattern and displacement vector and attenuation of horizontal displacement show that the significant changes are observed on accordance to the applied convergent displacement within the models. A series of model calculation have been carried out but only representative models are described here. The modeling results presented here based on: (i) σ_{Hmax} orientation, (i) Displacement vector and (iii) fault pattern.

6.2.1 σ_{Hmax} orientation

Figure 18 shows spatial distribution of the simulated σ_{Hmax} within the models. Fig. 18(a), 18(b) and 18(c) represent the σ_{Hmax} of model 1, 2 and 3 under boundary condition of BC 1, 2 and 3 respectively. Moreover, Fig. 18(d), Fig. 18(e) and Fig. 18(f) display the σ_{Hmax} orientation of model 4 with boundary condition 4, 5 and 6 respectively. Fig. 18(a) shows almost N-S directed σ_{Hmax} orientation with same magnitude within the model, and Fig. 18(b) shows considerable change in orientation and with small magnitude near the Dauki fault, Sylhet trough and the Shillong Plateau region. Fig. 18(c) indicates that the Bengal basin, the Shillong Plateau, the Brahmaputra valley, most part of the MBT show NE-SW orientation of stress whereas east of the Bengal basin and the Indo-Burmese Range show N-S orientation. Northeastern part of the model shows greater

magnitude of stress. Fig. 18(d) shows multi-directional stress orientation within the Bengal basin, the Shillong Plateau, Assam valley, Sylhet trough and the Dauki fault, but in southern part of the Shillong Plateau show NE σ_{Hmax} orientation. Area between the Meghna and the Jamuna fault and few parts of Assam valley and eastern part of the model (east of the Saigang fault) show N-S σ_{Hmax} orientation. Northern part of the model from the Brahmaputra fault (including the MBT), the eastern Bengal basin, the Indo-Burmese Range and northeastern Assam valley show NE orientation of σ_{Hmax} . Fig. 18(e) shows that σ_{Hmax} orientation within north of the MBT, the Indo-Burmese Range is NE but east of the Saigang fault region, there is N-S. The Shillong Plateau and the Brahmaputra valley show multi-directional stress orientation ENE-WSW to NW-SE. Vicinity of the Dauki fault show N-S σ_{Hmax} orientation that is not similar with entire the Bengal basin. However, few parts of the Indo-Burmese Range and eastern part of Bengal basin show NW-SE σ_{Hmax} orientation. Southwestern part of the Bengal basin shows very complex stress distribution. The magnitude of stress is different in different zones within this model. Fig. 18(f) shows similar stress orientation as seen in Fig. 18(d) of model 4 with boundary condition 4 without eastern part of the Bengal basin and some parts of the Indo-Burmese Range. These parts display N-S orientation of maximum compressive stress (σ_{Hmax}).



6.2.2 Displacement

We impose horizontal convergent displacement from the boundary of the model which implies the movement of every element within it and represent the velocity as a whole. A series of displacement were calculated under different boundary conditions and depth but we represent one representative of each model with each boundary condition under 1000m convergent displacement in Fig. 19 for 1 km depth. Fig. 19(a), Fig. 19(b) and Fig. 19(c) represent the displacement of model 1, 2 and 3 respectively. Fig. 19(d) Fig. 19(e) and Fig. 19(f) show the displacement of model 4 under boundary condition BC 4, BC 5 and BC 6 respectively. Fig. 19(a) shows the displacement in the western part of the Bengal basin and Himalayan Front region is NW-SE but middle and eastern part of the Bengal basin and the Indo-Burmese Range are N-S orientation. Northeastern part of the model 1 displays NE displacement with small magnitude. Fig. 19(b) shows similar NE displacement within the whole model and greater vector

displacement is observed in the southern part and gradually decreases toward north. ENE vector displacement is found within the Bengal basin, the Indo-Burmese Range, Assam, the Brahmaputra valley, the Naga-Mikir-hills region, and W-E displacement observed within the MBT in Fig. 19(c). In Fig. 19(d), we can see NE displacement in the entire Bengal basin, the Indo-Burmese Range, the Brahmaputra valley, the Naga-Mikir-hills region and the MBT (western part). North of the MBT and eastern part of the MBT show its displacement toward ENE with decreasing in magnitude toward the east. Fig. 19(e) shows multi-directional displacement within the model. The Sylhet trough, North of MBT and Brahmaputra valley show E-W displacement whereas eastern part of the Bengal basin exhibits NE displacement. Within the Indo-Burmese Range, and west of the Saigang fault show S-N displacement. In Fig. 19(f), we can see eastward displacement in the Bengal basin, the Brahmaputra valley, and north of the MBT, but rest of the model show NE displacement.

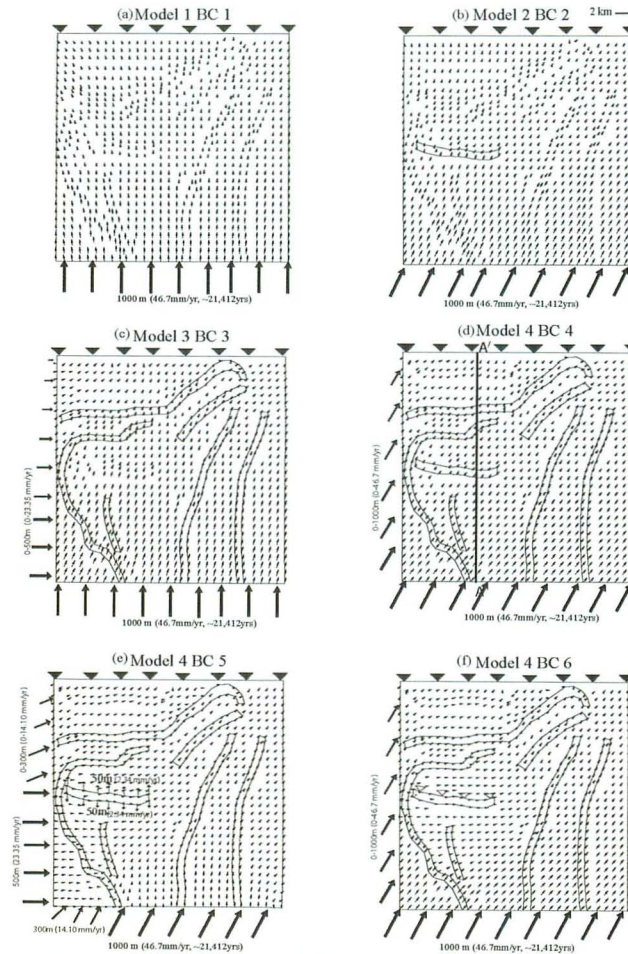


Fig. 19 Vector displacement for (a) model 1 with BC 1, (b) model 2 with BC 2, (c) model 3 with BC 3, (d) model 4 with BC 4, (e) model 4 with BC 5 and (f) model 4 with BC 6 under 1000 m convergent displacement.

6.2.3 Change of displacement within model

We analyse displacement rate of different model using different boundary condition. Fig. 20 shows change in displacement rate within the model 4 with boundary condition BC 4. The result suggested that ~25% (from 27 mm/yr to 17.5 mm/yr) velocity is reduced (along 91°E) due to presence of the prominent Dauki fault while the Brahmaputra fault and the MBT also reduce significant velocity. To produce Fig. 20, amount of net displacement of each node along A-A' (Fig. 19(d)) is taken from calculated data, and we convert it into displacement rate.

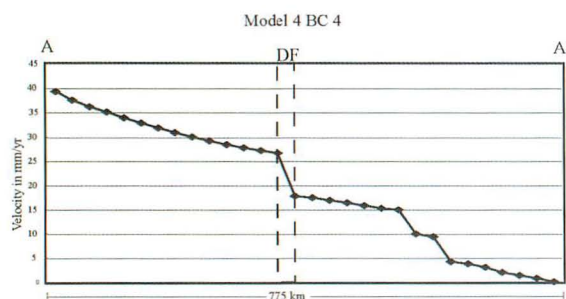


Fig. 20 N-S velocity attenuation within the model 4 under BC 4 along 91°E .

6.2.4 Model faulting

Fig. 21 shows a change in faulting pattern of the model 4 in term of depth variations. We simulate this model with depth of 1, 10 and 50 km (Fig. 21(a-c)) and found that faulting pattern does not change significantly with depth. Southern part of the Bengal basin and Tripura region show strike-slip faulting. The periphery of the Dauki fault including the Shillong Plateau displays strike-slip faults, whereas, eastern part of this fault indicate thrust faults. In contrast, the Brahmaputra valley shows thrust fault regime with strike-slip component. Northern part of the Indo-Burmese Range exhibits combination of thrust and strike-slip faults.

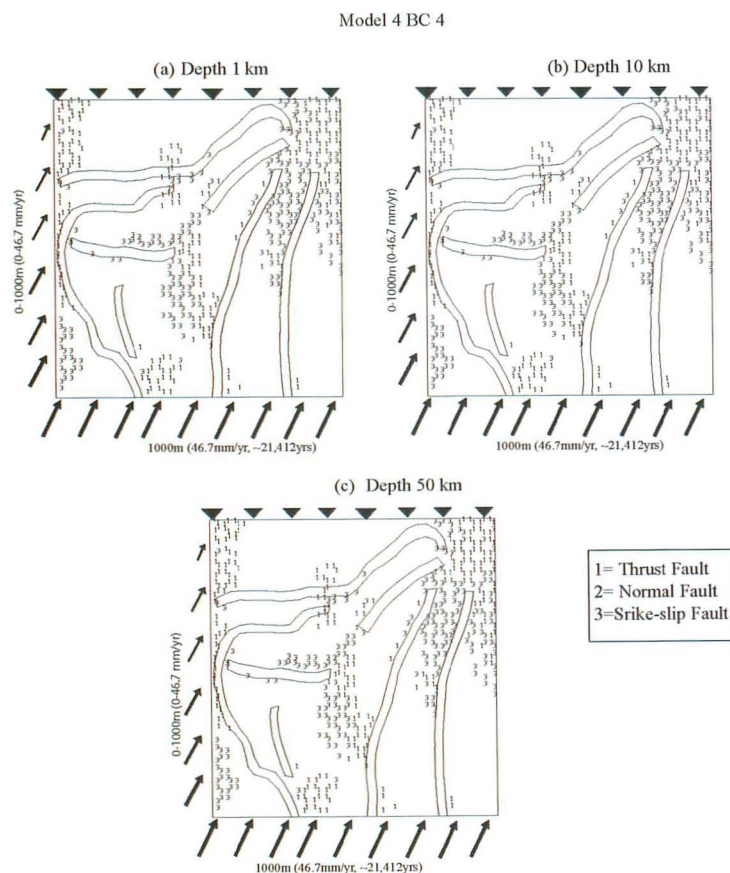


Fig. 21 Faulting pattern of the model 4 with BC 4 at depth of (1) 1 km (2) 10 km and (3) 50 km. 1, 2 and 3 indicates for thrust, normal and strike-slip faulting respectively.

6 Discussion

7.1. Discussion of plane strain case (I)

Some of the tectonic models have been studied to understand deformation within the Shillong Plateau and its adjoining regions (e.g., Bilham and England, 2001; Kayal et al., 2006, Clark and Bilham, 2008). Among these, the proposed 'pop up' tectonic model by Bilham and England (2001) is discussed most, and a controversy raised on the boundary faults. The existence of the proposed Oldham fault has a vital role on the regional deformation. We assessed this 'pop up' model using the cross-section model of Bilham and England (2001). We further compare my result with the regional tectonic stress, seismicity, focal mechanisms of earthquakes and other geophysical results.

The study area is tectonically much active, and is associated with the compressive stress regime (Gowd et al., 1992). In the Bengal basin, the orientation of maximum principal stress in the sedimentary pile is parallel to local E-W trend of convergent of Indo-Australia and west-Pacific plate relating to subduction zone forces (Rajendran et al., 1992). Prominent north trending folds and thrusts involving Pleistocene sediments in the eastern part of Bengal basin is also an indicator of E-W compression. Gowd et

al. (1992) reported that the P axes of earthquakes at the basement and crust below the Bengal basin are not similar to that prevailing in the Mid-continental stress province, that generally direct in N-NNW. The Assam valley area has no constant direction of maximum principal stress as the area is subducting beneath the syntaxial collision boundary (Rajendran et al., 1992). One strong earthquake M 5.8 in December 1984 shook the Silchar area of southern Assam that produced numerous ground cracks and these cracks are associated with an ENE trending P axis (Gowd et al., 1992). The sedimentary pile of Bengal basin is compressed by the westward push of overriding southern Indo-Burmese ranges resulting E-W compressive stress, whereas the basement and the crust beneath the Bengal basin show the same stress direction (E-W) as observed beneath the Shillong Plateau and farther north. Our simulated results reveal that the compressive stress regime exists within the Bengal basin, Assam and deeper part of the Shillong Plateau. The best-fit model (model 4 under BC-1) shows that a significant tensional stress regime exists within the upper part of the Shillong Plateau and Assam at shallower depth (< 25 km) (Fig. 22).

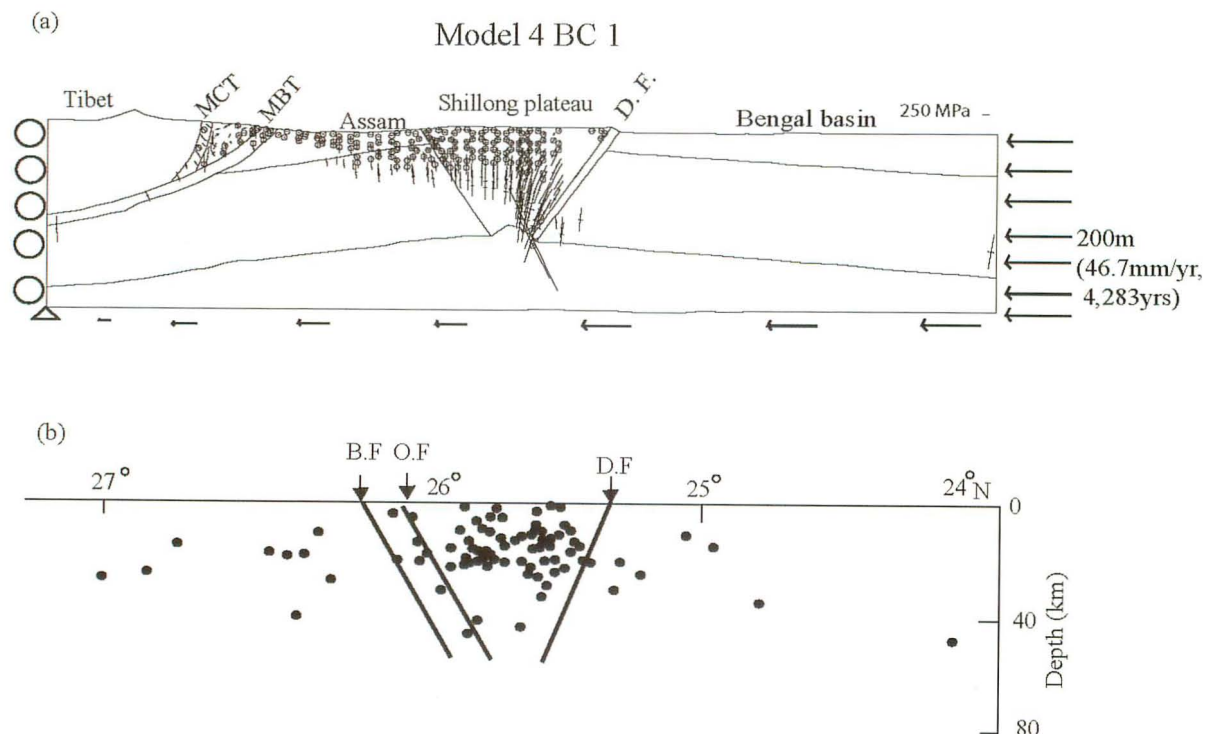


Fig. 22 Comparison between (a) principal stress within failure elements of model 4 under BC-1 and (b) depth of earthquakes (Nayak et al., 2008).

The earthquake records reveal that the Shillong Plateau and its surrounding areas are natural laboratories with high seismic activity, and a number of lineaments/faults are recognized in the Shillong Plateau. Several large earthquakes $M > 7$ are recorded in the northeastern Himalaya region in the past 110 yrs since the great 1897 Shillong Plateau earthquake (M 8.7). Rajendran et al. (2004) reported that during 1986-1999, most of the earthquakes occurred in the Shillong Plateau and in regions to its north in the Assam-Brahmaputra valley. They also reported that the earthquake is at < 30 km. The southern boundary Daspi thrust and the northern boundary south-dipping Brahmaputra fault are responsible for generating these earthquakes (Kayal et al., 2006). Seismic events in the Bengal basin (Fig. 22b) normally occur at the base of lower crust by strike-slip faulting at deeper depth ~ 48 -55 km (Khan and Hoque, 2006). The thick (~ 20 km) sediments in the Bengal basin is well reflected as low V_p (Bhattacharya et al., 2008).

Few deeper (depth > 30 km) earthquakes are located in Assam and Bengal basin around longitude 92°E with higher intensities (Verma, 1991). This longitudinal line is the eastern boundary of the Sylhet trough in Bengal basin. In the area south of the Dauki fault, the occurrence of shallow and deep earthquakes are related to the Sylhet trough (Das et al., 1995).

It is suggested that seismic stresses from the Himalayan arc to the north and from the Burmese arc to the east are transmitted to the Shillong Plateau (e.g. Mukhopadhyay, 1984; Kayal and De 1991; Kayal, 2001), and high level of microearthquake activity is recorded. The relocated epicenters by 3D inversion method demonstrate higher V_p and cluster of earthquake epicenters beneath the Shillong Plateau (Bhattacharya et al., 2008).

Earthquake focal mechanism solutions in or near the Shillong-Mikir hills-Assam valley reveals that the N-S compression is mostly dominant (Chen and Molnar, 1990; Bhattacharya et al., 2008) whereas Verma (1991) showed that Shillong Plateau has been subjected to N-S, NW-SE and NE-SW compressional stresses. Kayal et al. (2006) reported that the Shillong Plateau area is dominated by thrust faulting and the earthquakes are mostly confined within a depth of ~ 35 km (Fig. 21b).

Choudhury (2008) also analyzed very recent (2002-2008) earthquakes in and around Bangladesh and reported that this region is in strike-slip regime.

Our simulated distribution of failure elements show faulting pattern of the study area. The model 1 and model 4 (Fig. 11) are show that Dauki fault is a thrust faulting sense of movement. Kayal et al. (2006), however, called this segment of the Dauki fault as the Dapsi thrust. The model 2 shows thrust faulting with strike-slip component at depth. The best-fit model (model 4 under BC-1) infers the Dauki fault as a thrust fault and a few conjugate normal faults are associated with it (Fig. 22a). The best-fit model, however, does not describe the Bengal basin clearly. Our modeling results show some deeper failures within the Dauki fault. The distribution of failure elements are in agreement with the recent seismological data of Kayal et al. (2006).

In this modeling, we observed thrust faults and non-vertical maximum principal stress orientation within the eastern Himalaya and Tibet region, which is much consistent with regional tectonics. MBT and MCT always show thrust faults within our models and also observed few normal faults between these two faults. We overlook the results of this regions since our concerning area is Shillong Plateau and it's adjacent.

7.2 Discussion of plane stress case (II)

The tectonics and deformation pattern in southeastern India is complex due to differential movement of plates within the area (Kayal et al., 2006). We critically examine all modeling results (σ_{Hmax} orientation and vector displacement) and select model 4 using boundary condition 4 BC 4 is the best fit model (fig. 17d and 18d) because the model can explain the realistic Neotectonic events of the study area. We describe the tectonics and implication focusing the model results of (1) σ_{Hmax} of the study area, and (2) focal mechanism solution and nature of faulting.

7.2.1 σ_{Hmax} of the study area

We analyzes the previous studies (e.g. Chen and Molnar, 1990; Kayal and De, 1991; Ben-Menahem et al., 1974; Gowd et al., 1992; Islam, 2003; Choudhury, 2008; Khan and Chouhan, 1996; Bhattacharya et al.,

2008 and Rajendran et al., 1992) about fault-plane solution for understanding the present-day stress distribution within the study area. Figure 23 shows observed σ_{Hmax} orientation and major tectonic features in the Bengal basin and its surrounding area. E-W σ_{Hmax} orientation is existed in the upper part of the Bengal basin, south of the Dauki fault. The folded region of eastern part of Bangladesh, Tripura and Indo-Burmese Range indicate that the entire Bengal basin may be under E-W compression but earthquake data within the basement beneath the Bengal basin indicate generally N/NNE –S/SSW compression (Gowd et al., 1992). Khan and Couhan (1996) reported the consistent compressive stress orientation of the earthquake event within the Bengal basin which is NNE-SSW. Moreover, Bhattacharya et al. (2008) represent a combined fault-plane solution of previous studies (Chen and Molnar, 1990; Kayal and De, 1991 and Ben-Menahem et al., 1974) of the study area and show that σ_{Hmax} orientation is almost N-S in the entire study areas but eastern parts of the Bengal basin and the Indo-Burmese Range area with NE-SW direction. Chen and Molnar (1990) interpreted eight fault-plane solutions of earthquake of the Shillong-Mikir hills and Assam valley region that indicates NNE-SSW σ_{Hmax} . Different σ_{Hmax} orientation were found at places within Assam, Naga-Disang thrust folded belt and the Himalayan boundary, from bore breakouts and focal mechanism solution which suggest complex stress condition (Gowd et al., 1992). They also reported that the Mikir hills show its σ_{Hmax} orientation is N18°E and N64°E for the Indo-Burmese Range. However it is found that σ_{Hmax} orientation along the Himalayan front arc region is N-S and NNE-SSW whereas Assam syntaxis and Burmese Arakan Yoma are show NE-SW and E-W respectively (Rajendran et al., 1992). The recent studies (Islam, 2002; Choudhury, 2008) based upon a seismicity of 1977-2008 in the Bengal basin and its adjoining area is suggested that σ_{Hmax} orientation is NE-SW. In the contrary, Angelier and Baruah (2009) studied 245 focal mechanism solution of the study area and reported N-S compression in the eastern Himalaya to the Bengal basin through Shillong Plateau -Mikir Hills-upper Assam valley.

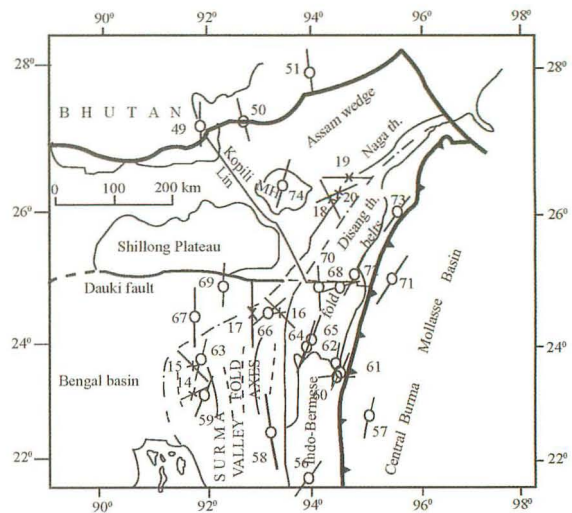


Fig. 23 σ_{Hmax} orientation of the study area (modified after Gowd et al., 1992).

In the World Stress Map (Fig. 24), we can find that no stress data is available within the western part of the Bengal basin. Folded part of the Bengal basin and Tripura are show σ_{Hmax} trending E-W and NE orientation. In the other hand, northwestern the Indo-Burmese Range and northern part of Tripura show NE σ_{Hmax} orientation while the eastern part of the Indo-Burmese Range shows E-W σ_{Hmax} orientation. The Shillong Plateau region shows NE orientation of σ_{Hmax} whereas northeastern part of Brahmaputra valley show NE, E-W and NW-SE in bore breakout. The MBT and northwest of it show NW and sometimes NE σ_{Hmax} orientation.

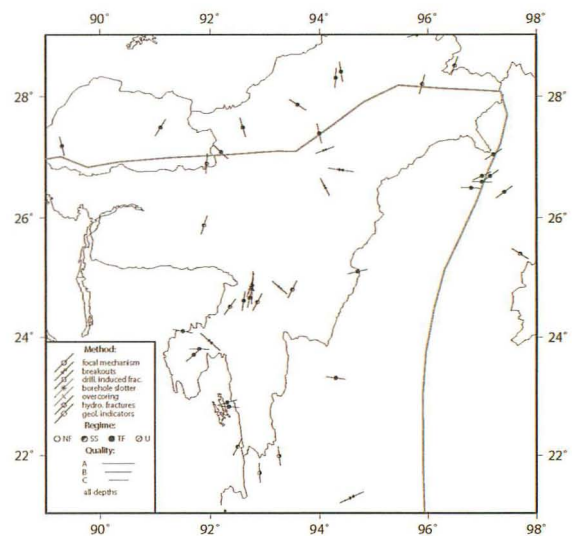


Fig. 24 World Stress Map (CASMO, 2009)

Our computed model results (Fig. 25) show that σ_{Hmax} orientation took a multi-directional in the Bengal basin, the Shillong Plateau and Assam region. Sylhet trough, the Dauki fault and southern part of the Shillong Plateau show NE σ_{Hmax} orientation. Areas between the Meghna and the Jamuna lineament and few parts of Assam region show N-S σ_{Hmax} orientation. Northern part of the model from the Brahmaputra lineament (including the MBT), the eastern Bengal basin, the Indo-Burmese Range and northeastern Assam valley show NE σ_{Hmax} orientation while the east of the Saigang fault shows N-S σ_{Hmax} orientation.

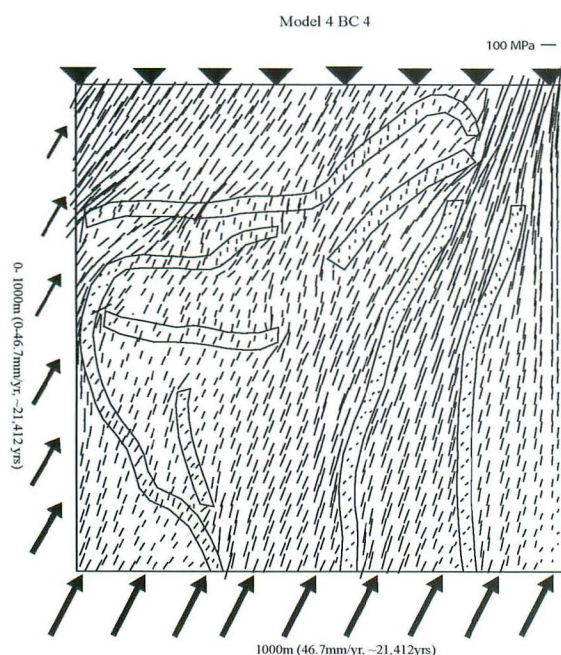


Fig. 25 σ_{Hmax} orientation of the study area from the modeling (model 4 with BC 4).

7.2.2 Focal Mechanism Solution and nature of faulting

Chen and Molnar (1990) studied 17 earthquake events occurred in and around the Shillong Plateau, the Bengal basin and the northern Indo-Burmese Range which is shown in Fig. 26. The Assam- Shillong Plateau -Mikir hills area, N-S compressive stress is dominants in all events (events 1-6 in Fig. 26) on focal mechanism solution. Event 4 shows thrust faulting and represents the faulting pattern within the Brahmaputra valley, whereas, other five events are strike-slip faulting. On the other hand, Kayal and De (1991) presented four composite focal mechanism solutions (A-D in Fig. 26) from four cluster of events that were

recorded in temporary micro-seismicity network located in the Shillong Plateau -Mikir-hills area, and all these solution indicates reverse faulting with strike-slip component (Bhattacharya et al., 2008). Kayal et al. (2006) stated that the Shillong Plateau area is dominated by thrust faulting.

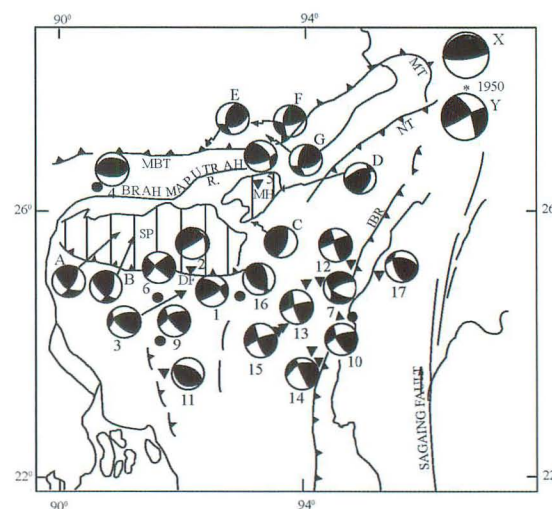


Fig. 26 Fault-plane solutions of earthquakes in NE India region (Modified after Bhattacharya et al., 2008). NT-Naga-Thrust, IBR-Indo-Burmese Ranges, SP-Shillong Plateau, MBT-Main Boundary Thrust, MH-Mikir Hills, DF-Dauki fault. Solid circles and solid rectangles indicate the seismic station.

Chen and Molnar (1990) reported eight focal mechanism solutions in and adjacent to the Indo-Burmese Range (events 7, 10, 12, 13, 14, 15, 16 and 17) that characterized by a combination of reverse and strike-slip faulting with NNE-SSW compressional stress (Fig. 26). Ni et al. (1989) inferred that the Sagaing fault and Kaladan fault are right-lateral strike-slip faulting in nature throughout the collision history in the complex convergent marginal zone. The focal mechanism solution of event 9 in the Bengal basin shows reverse faults with strike-slip motion but event (event 11) in Tripura folded belt shows pure reverse faults (Bhattacharya, 2008). Khan and Chouhan (1996) studied 12 earthquake events during 1968-1989 of the Bengal basin and they reported that all events associated with strike-slip faulting with thrust component. Choudhury (2008) also studied very recent (2002-2008) earthquakes events in and around Bangladesh, and reports that all events are associated with strike-slip fault. The earthquakes events occurred <30 km focal depth are mostly associated with subduction tectonics in the Indo-Burmese Range and

the Jamuna lineament (Hoque and Khan, 2006). They also inferred suggested that the Dauki fault area is the weak zones of strain accumulation owing to lack of energy release. Recently, Angelier and Baruah (2009) published their huge focal mechanism solution study (Fig. 27) which is consistent with previous study and they also show complex faulting pattern within Indo-Burmese area. Eastern part of Bangladesh (Chittagong) and some part of Tripura region show thrust type of faulting whereas strike slip faults are found further east in the World Stress Map (Fig. 24). In this map, the Shillong Plateau shows strike-slip faults but the MBT, the Brahmaputra valley and north of it show thrust faults.

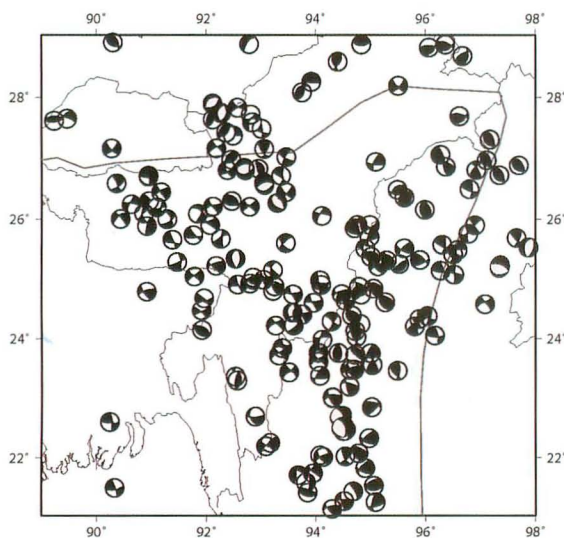


Fig. 27 Focal mechanism solution of the study area (modified after Angielier and Baruah, 2009).

In our result of model 4 (BC-4) with depth of 1, 10 and 50 km (Fig. 21(a-c)), show fault pattern does not change significantly with depth and this model is consistent with the natural and realistic faults in the study area. Southern part of the Bengal basin, the Dauki fault, the Shillong Plateau and Tripura region show strike-slip fault, and eastern part of the Dauki fault shows thrust faults. Moreover, the Brahmaputra valley shows thrust faults with strike-slip component and northern part of the Indo-Burmese Range exhibits combination of thrusts and strike-slip faults.

In addition, our models imposed boundary condition of BC 5 and BC 6 (Fig. 9(e) and 9(f)) for different thinking (either the Dauki fault is a drifting region or accommodate total northward local

movement from southern part) give reasonable vector displacement (Fig. 18(e) and 18(f)), however σ_{Hmax} orientation is result (Fig. 17(e) and 17(f)) within the Bengal basin and the Brahmaputra valley including the Shillong Plateau is not satisfactory. Finally, we can say that the Dauki fault zone is not either under continental drift or does not accommodate total local displacement there except experiencing regional compression and accommodating strain.

8 Conclusions

The FE modeling explains the present-day stress field and deformation style in the Shillong Plateau and adjoining areas in northeast India and Bangladesh (Bengal basin). Our plane strain models are based on the initial pop up model of the Shillong Plateau given by Bilham and England (2001). The simulated results are compared with the seismic activity and faulting. We propose model 4 with BC 1 is the best-fit model which having realistic stress field and represent natural failure pattern in the Shillong Plateau and its adjoining areas. The results show that the Bengal basin and Assam-Brahmaputra valley are under compressive stress regime. Upper part of the Shillong Plateau, however, shows tensional stress regime, but deeper part indicates compressive stress regime. The greater value of maximum shear stress is observed at the bottom of crust beneath the Shillong Plateau and at the Dauki fault zone that indicates considerable stress accumulation between interseismic periods. Some of this stress energy may be released through microseismic activity but most of energy is released only through larger earthquakes. Lower value of principal stresses in the fault zones may imply an accommodation of regional deformation within these zones. With an increase convergence displacement, the Assam-Brahmaputra valley and upper part of the Bengal basin show anticlockwise rotation of principal stresses which characterizes thrust faulting under the existing tectonic environment. The upper part of the Shillong Plateau region shows the normal faulting under tensional stress condition. The Oldham fault at the northern boundary of the Shillong Plateau is not evident as a structural discontinuity in the best-fit

model that indicates our modeling result is not favor the existence of Oldham fault at northern boundary of the Shillong Plateau. The best-fit model also does not support the pop-up of the Shillong Plateau and is suggested that the Plateau is mainly due to plate convergence.

In plane stress models, we simulate the horizontal maximum compressive stress (σ_{Hmax}) of the Bengal basin, the Shillong Plateau, Assam, the Indo-Burmese Range and adjoining areas to explain the neotectonic activity within these areas. Our preferred best-fit model (model 4 with BC 4) explains that the study area has complex stress orientation. The southern Bengal basin and east of the Saigang fault area shows N-S σ_{Hmax} orientation but rest of the areas show NE-SW orientation. It is evident that our simulated results able to explain the σ_{Hmax} orientation of the central-part of the Bengal basin, Tripura folded belt, the Shillong Plateau, Himalayan front including the MBT, the Indo-Burmes Range properly but have some anomaly to describe the area of upper Assam. The entire Bengal basin, the Indo-Burmese Range, the Brahmaputra valley, the Naga-Mikir hills, western part of the MBT show the regional NE displacement within my best-fit model while eastern part of the MBT and north of the MBT show NNE velocity. It is also found in our modeling results that the convergent displacement is gradually decreases from the south to north. In addition, we also observe that ~25% convergent displacement within the model is accommodated by the Dauki fault (Fig. 20) alone and this fault is the major controlling element of regional deformation velocity as well as stress distribution. Besides, we also determine the fault pattern of the study area considering different rock parameters (density, Young's modulus, Poisson's ratio, internal angle friction etc.) and Mohr-Coulomb failure criterion which shows that southern part of the Bengal basin, Tripura and the Dauki fault region show strike-slip faults. On the other hand, Brahmaputra valley displays thrust faults with strike-slip component but the Indo- Burmese Range exhibits combination of thrust and strike-slip faulting. In comparison to previous studies (Chen and Molnar, 1990; Kayal et al., 2006; Bhattacharya et al., 2008), our preferred model results show consistent faults pattern that enable to

explain the study area more realistically.

Acknowledgement

M. S. I. is grateful to Ministry of Education, Culture, Sports, Science and Technology (Monbukagakusho) Japan for providing scholarship to carry out this research fruitfully under Okinawa International Marine Science Program of the Graduate School of Engineering and Science, University of the Ryukyus, Okinawa, Japan.

References

- Acharyya, S. K., 2007. Collisional emplacement history of the Naga-Andaman ophiolites and the position of the eastern India suture. *Journal of Asian Earth Science*, **29**, 229-242.
- Alam, M., 1989. Geology and depositional of Cenozoic sediments of Bengal Basin of Bangladesh. *Paleogeogr. Paleoclimatol. Paleocol.*, **69**, 125-139.
- Alam, M., Alam, M.M., Currey, J.R., Chowdhury, M.L.R. and Gani, M.R., 2003. An overview of the sedimentary geology of the Bengal Basin relation to the regional tectonic framework and basin-fill history. *Sedimentary Geology*, **155**, 179-208.
- Angeiler, J and Baruah, S., 2009. Seismotectonics in Northeast India: a stress analysis of focal mechanism solution of earthquakes and its kinematic implications. *Geophysical Journal International*,
doi:10.1111/j.1365-246X.2009.04107.x.
- Ben-Menahem, A., Aboudi, E., Schild, R., 1974. The source of the great Assam earthquake-an intraplate wedge motion. *Physics of Earth and Planetary Interior* **9**, 265-289.
- Bhattacharya, P.M., Mukhopadhyay, S., Majumdar, R.K. and Kayal, J.R., 2008. 3-D seismic structure

- of the northeast India region and its implication for local and regional tectonics. *Journal of Asian Earth Science*, **33**, 25-41.
- Bilham, R. and England, P., 2001. Plateau 'pop up' in the great 1897 Assam earthquake. *Nature*, **410**, 806-809.
- Biswas, S. and Grasemann, B., 2005. Quantitative morphotectonics of the southern Shillong Plateau (Bangladesh/India), *Aus. J. Earth Sci.*, **97**, 82-93.
- Biswas, S., Coutand, I., Grujic, D., Hager, C., Stocklin, D. and Grasemann, B., 2007. Exhumation and upliftment of the Shillong plateau and its influence on the eastern Himalayas; New constraints from the apatite and zircon (U-Th- Sm)/He and apatite fission track analyses. *Tectonics*, **26**, TC6013, doi:10.1029/2007TC002125.
- Chen, P. and Molnar, P., 1990. Source parameters of Earthquakes and Interplate Deformation Beneath the Shillong Plateau and the Northern Indoburman Ranges. *J. Geophys. Res.*, **95**, 12527-12552.
- Chen, Z., Burchfiel, B.C., Liu, Y., King, R.W., Royden, L.H., Tang, W., Wang, E., Zhao, J. and Zhang, X., 2000. Global Positioning System measurements from eastern Tibet and their implications for India/Eurasia intercontinental deformation. *J. Geophys. Res.*, **105**, 16215-16227.
- Clark, M.K. and Bilham, R., 2008. Miocene rise of the Shillong Plateau and the beginning of the end for the Eastern Himalaya. *Earth and Planetary Science Letters*, **269**, 337-351.
- Clark, JR. S.P.R., 1966. *Handbook of Physical Constants*. Geol. Soc. Am., Mem., 587p.
- Choudhury, S.A., 2008. Moment tensor and hypocenter determination using waveform data from the new Bangladesh seismic network. M. Sc thesis, IISSE, Tsukuba, Japan. P1-6.
- Curry, J.R., Moore, D.G., 1974. Sedimentary and tectonic processes in Bengal deep-sea fan and geosyncline. In: Burk, C.A., Drake, C.L. (Eds.), *The Geology of Continental Margins*. Springer-Verlag, New York, pp. 617- 628.
- Das, J.D., Saraf, A.K. and Jain, A.K., 1995. Fault tectonics of the shillong plateau and adjoining regions, north-east India using remote sensing data. *International Journal of Remote Sensing*, **16**, No. 9, 1633-1646.
- DeMets, C., Gordon, R.G., Argus, D.F. and Stien, S., 1994. Effect of Recent Revisions to the Geomagnetic Time Scale on Estimates of Current Plate Motion. *Geophys. Res. Lett.*, **21**, 2191-2194.
- Evans, P., 1964. The tectonic framework of Assam. *Journal of the Geological society of India* **5**, 80-96.
- Gordon, R.G., Argus, D.F., Heflin, M.B., 1999. Revised estimate of the angular velocity of India relative to Eurasia. *Eos. Trans. AGU* **80** (46) Fall Meet. Suppl., F273, San Francisco.
- Gowd, T. N. and Srirama Rao, S. V., 1992. Tectonic stress field in the Indian Subcontinent. *Journal of Geophysical Research*, **97**, NO. B8, 11879-11888.
- Gough, D. I., C. K. Fordjor, and J. S. Bell., 1983. A stress province boundary and tractions on the North American plate, *Nature*, **305**, 619-621.
- Hayashi, D., 2008. Theoretical basis of FE simulation software package. *Bull.Fac.Sci.univ.Ryukyus*, No.85, 81-95. (<http://ir.lib.u-ryukyu.ac.jp>)
- Hodges, H.V., 2000. Tectonics of the Himalaya and southern Tibet from two perspectives. *GSA Bulletin*, **112**, 324-350.
- Holt, W.E., Chamot-Rooke, N., Pichon, L.X., Shen-Tu, B., and Ren, J. Haines, A.J., 2000. Velocity field in Asia inferred from Quaternary fault slip rates and Global Positioning System observations.

- J. Geophys. Res., **105**, NO. B8, 19,185-19,209.
- Ingersoll, R.N., Graham, S.A., Dickinson, W.R., 1995. Remnant ocean basins. In: Busby, C.J., Ingersoll, R.V. (Eds.), *Tectonics of Sedimentary Basins*. Blackwell, Oxford, 363-391.
- Islam, M. M., 2003. Seismicity in Bangladesh using local seismic station. Individual Study Participant Institute of Seismological Earthquake Engineering, Tsukuba, Japan, 1-9.
- Jade, S., 2004. Estimates of plate velocity and crustal deformation in the Indian subcontinent using GPS geodesy, *Current Science*, **86**(10), 1443-1448.
- Jade, S., Mukul, M., Bhattacharyya, A.K., Vijayan, M.S.M., Jaganathan, S., Kumar, A., Tiwari, R.P., Kumar, A., Kalita, S., Sahu, S.C., Krishna, A.P., Gupta, S.S., Murthy, M.V.R.L., and Gaur, V.K., 2007. Estimate of interseismic deformation in Northeast India from GPS measurements. *Earth and Planetary Science Letters*, **263**, 221-234.
- Johnson, S.Y. and Alam, A.M.N., 1991. Sedimentation and tectonics of the Sylhet trough, Bangladesh. *Geological Society of America Bulletin*, **103**, 1513-1527.
- Kailasam, L.N., 1979. Plateau uplift in Peninsular India. *Tectonophysics*, **61**, 243-269.
- Kayal, J.R. and De, Reena., 1991. Microseismicity and tectonics in northeast India. *Bulletin of Seismological Society of America*, **77**, 1718-1727.
- Kayal, J.R., 2001. Microearthquake activity in some parts of the Himalaya and the tectonic model. *Tectonophysics*, **339**, 331-351.
- Kayal, J.R., Arefiev, S.S., Barua, S., Hazarika, D., Gogoi, N., Kumar, A., Chowdhury, S.N. and Kalita, S., 2006. Shillong plateau earthquakes in northeast India region: complex tectonic model. *Current Science*, **91**, No.1, 109-114.
- Keary, P. and Frederick, J.F., 1998. *Global Tectonics*. Blackwell Science publishing company, p333.
- Kent, W.N., and Dasgupta, U., 2004. Structural evolution in response to fold and thrust belt tectonics in northern Assam. A key to hydrocarbon exploration in the Jaipur anticline area. *Marine and Petroleum Geology*, **21**, 85-803.
- Kent, R. W., Saunders, A. D., Kempton, P. D. and Ghose, A. C., 2002. $^{40}\text{Ar}/^{39}\text{Ar}$ geochronology of the Rajmahal basalts, India, and their relationship to Kerguelen Plateau. *Journal of Petrology*, **43**, 1141-1153.
- Khan, A.A. and Agarwal, B.N.P., 1993. The Crustal Structure of the western Bangladesh from gravity data. *Tectonophysics*, **219**, 341-353.
- Khan, A.A and Chouhan, R.K.S., 1996. The crustal dynamics and tectonic trend in the Bengal Basin. *Journal of Geodynamics*, **22**, 267-286.
- Khan, A.A. and Rahman, T., 1992. Analysis of the gravity field and tectonic evolution of the northwestern part of Bangladesh. *Tectonophysics*, **206**, 351-364.
- Khan, A.A and Sattar, G.S. and Rahman T., 1994. Tectonogenesis of the Gondwana rifted basin of Bangladesh in the so-called Garo-Rajmahal Gap and their pre-drift regional tectonic correlation. *Gondwana 9*, V.2, Geological survey of India, Oxford & IBH Pub., New Delhi, p647-655.
- Khan, A.A. and Hoque, M.A., 2006. Crustal Dynamics, Seismicity and Seismotectonics of the Bengal basin. Proc. 1st Bangladesh earthquake symp. Bangladesh Earthquake Society, 45-54.
- Krisna, M.R. and Sanu, T.D., 2000. Seismotectonics and rate of active crustal deformation in the Burmese arc and adjoining regions. *Journal of Geodynamics*, **30**, 401-421.

- Lohmann, H.H., 1995. On the tectonics of Bangladesh. Swiss Association of Petroleum. Geology and Engineering Bulletin, **62** (140), 29–48.
- Lee, T.T. and Lawver, L.A., 1995. Cenozoic plate reconstruction of Southeast Asia. Tectonophysics, **251**, 85-138.
- Macwell, S.J., Zimmerman, M.E. and Kohlstedt, D.L., 1998. High-temperature deformation of dry diabase with application to tectonics on Venus. J. Geophys. Res., **103**, 975-984.
- Malaimani, E.C., Campbell, J., Gorres, B., Kothoff, H. and Smaritschnik, S., 2000. Indian plate kinematics studies by GPS-geodesy. Letter of Earth Planet Space, **52**, 741-745.
- Mishra, U.K. and Sen, S., 2001. Dinosaur bones from Megalaya. *Current Science*, **80**, No. 8, 1053-1056.
- Mukhopadhyay, M., 1984. Seismotectonics of transverse lineaments in the eastern Himalaya and its foredeep. Tectonophysics, **109**, 227-240.
- Mukhopadhyay, M., Dasgupta, S., 1988. Deep structure and tectonics of the Burmese Arc: constraints from earthquake and gravity data. Tectonophysics **149**, 299–322.
- Nayak, G.K., Rao, V.K., Rambabu, H.V. and Kayal, J.R., 2008. Pop-up tectonics of the Shillong Plateau in the great 1897 earthquake (Ms 8.7): Insight from the gravity in conjunction with the recent seismological results. Tectonics, **27**, TC1018, doi:10.1029/2006TC002027.
- Ni, J.F., Guzma'n-Speziale, M., 1989. Accretionary tectonics of Burma and the three dimensional geometry of the Burma subduction zone. Geology **17**, 68– 71.
- Oldham, R.D., 1899. Reopt of the great earthquake of 12th June, 1897. *Mem. Geol. Surv. India*, **46**, 257-276.
- Paul, J., Burgmann, R., Gaur, V.K., Bilham, R., Larson, K.M., Ananda, M.B., Jade, S., Mukal, M., Anuama, T.S., Satyal, G. and Kimar, D., 2001. The motion and active deformation of India. Geophysical Research Letters, **28**, No. 4, 647-650.
- Rajasekhar, R.P. and Mishra, D.C., 2008. Crustal structure of Bengal Basin and Shillong Plateau: Extension of Eastern Ghat and Saatpura Mobile Belts to Himalyan fronts and seismotectonics. *Gondwana Research*, doi:10.1016/j.gr.2007.10.009.
- Rajendran, C.P., Rajendran, K., Daurah, B.P. and Earnest, A., 2004. Interpreting the style of faulting and paleoseismicity associated with the Shillong, northeast India, earthquake: Implication for regional tectonism. Tectonics, **23**, TC4009, doi:10.1029/2003TC001605.
- Rajendran, K., Talwani, P. and Gupta, H.K., 1992. State of stress in the Indian Subcontinent: A review. *Current Science*, **62**, Nos. 1&2. 86-93.
- Ray, S. J., Pattanayak, S. K. and Pande, K., 2005. Rapid emplacement of the Kerguelen plume-related Sylhet Traps, eastern India: Evidence from 40Ar-39Ar geochronology. Geophysical Research Letters, **32**, L10303, doi:10.1029/2005GL022586.
- Santosh, M., 1999. Integrated geological Studies in the Deep continental Crust of Southern India. *Gondwana Research*, **2**, No. 2. 309-310.
- Sella, G.F., Dixon, T.H., and Mao, A., 2002. REVEL: A model for the recent plate velocities from space geodesy. Journal of Geophysical Research, **107**, No. B4, 2081, doi:10.1029/2000JB000033.
- Shen, Z.K., Zhao, C., Yin, A., Li, Y., Jackson, D.D., Fang, P. and Dong, D., 2000. Contemporary crustal deformation in east Asia constrained from Global Positioning System measurements. J. Geophys. Res., **105**, 5721-5734.

- Socquet, A., Vigny, C., Rooke, N.C., Simons, W., Rangin, C., Ambrosious, B., 2006. India and Sunda Plate Motion and Deformation along their Boundary in Myanmar Determined by GPS. *J. Geophys. Res.*, **111**, (B05406). doi:10.1029/2000JB000033.
- Srinivasan, V., 2003. Deciphering differential uplift in Shillong Plateau using remote sensing. *Jour. Geol. Soc. India*, **62**, 773-777.
- Verma, R.K. and Mukhopadhyay, M., 1977. An Analysis of the Gravity field in northeastern India. *Tectonophysics*, **42**, 283-317.
- Verma, R. K., M. Mukhopadhyay, and Ahluwalia, M. S., 1976. Seismicity, gravity and tectonics of north east India and northern Burma, *Bulletin of Seismological Society of America*, **66**, 1683-1694.
- Verma, R.K., 1991. Seismicity of the Himalaya and the northeast India, and nature of continent-continent collision. In *Geology and Geodynamics Evolution of the Himalyan Collision Zone, part 2*, edited by K. K. Sharma (Oxford: Pergamon Press) 18, pp345-370.
- Yeats, R. S. and Thakur, V. C., 2008. Active faulting south of the Himalayan front: Establishing a new plate boundary. *Tectonophysics*, **453**, 63-73.